DESIGN OF DEPLOYABLE STRUCTURES COMPRISING ALTMANN LINKAGES

A Thesis Submitted to the

Graduate School of Engineering and Sciences of

İzmir Institute of Technology

in Partial Fulfillment of the Requirements for the Degree of

MASTER OF SCIENCE

in Mechanical Engineering

by

Görkem YILDIZ

December 2020

İZMİR

ACKNOWLEDGMENTS

First of all, I would like to give my sincere thanks to my advisor, Dr. Gökhan KİPER for his recommendations, support, motivation and encouragement during my thesis.

I am grateful to all members of Rasim Alizade Mechatronics Laboratory for their motivation.

I would like to thank the members of my thesis examining committee; Dr. Koray KORKMAZ and Dr. Erkin GEZGİN for their invaluable suggestions to complete this thesis.

I am also deeply grateful to CMS Jant ve Makine San. A.Ş. and my colleagues there for their support and patience during my thesis.

Lastly but most importantly, I would like to express my deepest appreciation to my sister Gizem YILDIZ, my father Teoman YILDIZ, my mother Nuray YILDIZ and Hatice SANDALLI for their love, never-ending support and patience during my education.

ABSTRACT

DESIGN OF DEPLOYABLE STRUCTURES COMPRISING ALTMANN LINKAGES

The main objective of this thesis is to investigate possible mobile networks comprising modified Altmann linkages which can be used as deployable structures. Altmann linkage is an overconstrained single-loop linkage with six revolute joints. Within the scope of this thesis, first a modified version of the Altmann linkage is introduced. The modified version of the linkage allows more feasible solutions for constructional design compared to the original linkage. Then, the loop closure equations are written and input/output relationship of the linkage are obtained. Next, possible networks of modified Altman linkages are examined. The networks are obtained either by taking two common links between adjacent loops, or connecting adjacent loops with two new revolute joints without any common links. Also, mobility analysis is performed for each network. Finally, the deployment stages of obtained networks are modelled in a CAD software. Some of the derived networks are already noted in the literature, but several novel networks are introduced in this thesis.

ÖZET

ALTMANN MEKANİZMALARI İÇEREN KATLANABİLİR YAPILARIN TASARIMI

Bu tezin temel amacı katlanabilir yapılarda kullanılabilecek modifiye edilmiş Altmann mekanizmalarından oluşan mekanizma ağlarını incelemektir. Altmann mekanizması, altı döner mafsal içeren fazla kısıtlı, tek devreli bir çubuk mekanizmasıdır. Tez kapsamında ilk olarak modifiye edilmiş Altmann mekanizması sunulmuştur. Modifiye edilmiş Altmann mekanizması, orijinal mekanizmaya göre daha basit konstrüksiyonel tasarıma elverişlidir. Mekanizmanın devre kapalılık denklemleri ile girdi/çıktı denklemleri çıkarılmıştır. Daha sonra, olası mekanizma ağları incelenmiştir. Mekanizma ağları iki şekilde elde edilmiştir: 1) iki komşu devrede iki ortak uzuv kullanılarak; 2) ortak uzuv olmaksızın iki komşu devre iki döner mafsalla bağlanarak. Ayrıca elde edilen her mekanizma ağının serbestlik derecesi belirlenmiş ve her bir ağ katı modelleme programında modellenerek hareketi incelenmiştir. Elde edilen mekanizma ağlarından bazıları literatürde mevcut olmakla birlikte bu tezde pek çok yeni mekanizma ağları sunulmuştur.

TABLE OF CONTENTS

LIST OF FIGURES vii

LIST OF TABLES x

CHAPTER 1. INTRODUCTION 1

1.1. Overconstrained Linkages 3

1.1.1. 4*R* Bennett Linkage 3

1.1.2. 5*R* Linkages 6

1.1.3. 6*R* Linkages 8

1.1.3.1. Sarrus Linkage 8

1.1.3.2. Altmann Linkage 9

1.2. Aim and Scope 11

CHAPTER 2. MODIFIED ALTMANN LINKAGE 12

CHAPTER 3. DEPLOYABLE STRUCTURES COMPRISING MODIFIED ALTMANN LINKAGES 24

3.1. Network of Modified Altmann Linkages with Common Links or Joints 24

3.1.1. Common Bar & Hub Case (Arch Version) 25

3.1.2. Common Two Bars Case (Scissor-like Version) 27

3.1.2.1. Connection of Long Link to Short Link 27

3.1.2.2. Connection of Short Link to Short Link (or Long Link to Long Link) 29

3.1.2.3. Connection of Long Link to Short Link with a Kink Angle . 30

3.1.2.4. Connection of Short Link to Short Link (or Long Link to Long Link) with a Kink Angle 31

3.1.3. One Common Bar & One Common Hub – New Version 32

3.1.3.1. Common Long Link and Hub 33

3.1.3.2. Common Short Link and Hub 34

3.1.4. Four Loops with a Common Hub (Dome version) 35

3.2. Network of Altmann Linkages with Two New Joints 37

3.2.1. Altmann Loop Version 38

3.2.2. Parallelogram Loop Version 40
3.2.2.1. Connection of Long Link to Short Link 41
3.2.2.2. Connection of Short Link to Short Link 42
3.2.3. 4-Loop Version 44

CHAPTER 4. CONCLUSION 46

REFERENCES 48

LIST OF FIGURES

Figure **Page**

Figure 1.1 Denavit-Hartenberg patameters (Source: Chen 2003) 2
Figure 1.2. Schematic diagram of the Bennett linkage (Source: Chen 2003)..... 4
Figure 1.3. Bennet Network of Chen (Source: Chen 2003)..... 6
Figure 1.4. Goldberg (a) 5R Linkage, (b) 6R Linkage (Source: Goldberg 1943) 7
Figure 1.5. Myard linkage (Source: Kiper 2018)..... 7
Figure 1.6. Sarrus linkage, (a) Bennet's Model, (b) schematic diagram (Source: Chen 2003) 8
Figure 1.7. Altmann linkage (modified from (Baker 1993)) 9
Figure 1.8.(a) Schematic of an Altmann Linkage, (b) A deployable network constructed by Altmann linkages (Source: Song et al. 2016) 10
Figure 1.9. Model of a modified Altmann linkage (Source: Atarer, Korkmaz, and Kiper 2017) 10
Figure 2.1. Schematic representation of the modified Altmann linkage 12
Figure 2.2. Attached reference frames to the modified Altmann linkage..... 13
Figure 2.3. Modified Altmann linkage 14
Figure 2.4. Assembly modes of a modified Altmann linkage 19
Figure 2.5. Output angle verification of assembly modes of a modified Altmann linkage 20
Figure 2.6. Input (θ_2)/output (θ_1) relationship when a = b..... 21
Figure 2.7. Input (θ_2)/output (θ_3) relationship when a = b..... 21
Figure 2.8. Input (θ_2)/output (θ_1) relationship when a = 1.5b..... 22
Figure 2.9. Input (θ_2)/output (θ_3) relationship when a = 1.5b..... 22
Figure 2.10. Input (θ_2)/output (θ_1) relationship when a = 2b..... 23
Figure 2.11. Input (θ_2)/output (θ_3) relationship when a = 2b..... 23
Figure 3.1. Schematic diagram of arch version 26
Figure 3.2. Deployed stage of arch version 26
Figure 3.3. Semi-deployed and folded stages of arch version 26
Figure 3.4. Schematic diagram of long link to short link connection..... 28
Figure 3.5. Deployed stage of long link to short link connection..... 28
Figure 3.6. Semi-deployed and folded stages of long link to short link connection..... 28

Figure **Page**

Figure 3.7. Schematic diagram of short link to short link connection 29
Figure 3.8. Deployed stage of short link to short link connection 29
Figure 3.9. Semi-deployed and folded stages of short link to short link connection 29
Figure 3.10. Schematic diagram of long link to short link connection with a kink angle 30
Figure 3.11. Deployed stage of long link to short link connection with a kink angle 30
Figure 3.12. Semi-deployed stage of long link to short link connection with a kink angle 30
Figure 3.13. Schematic diagram of short link to short link connection with a kink angle 31
Figure 3.14. Deployed and semi deployed stages of short link to short link connection with a kink angle - with equivalent angulated elements 31
Figure 3.15. Deployed and semi-deployed stages of short link to short link connection with a kink angle - with mirror-image angulated elements 32
Figure 3.16. Schematic diagram of common long link and hub version 33
Figure 3.17. Deployed stage of common long link and hub version 33
Figure 3.18. Semi-deployed stage of common long link and hub version 33
Figure 3.19. Front view of folded stage of common long link and hub version 34
Figure 3.20. Top view of folded stage of common long link and a hub version 34
Figure 3.21. Schematic diagram of common short common link and hub version 34
Figure 3.22. Deployed stage of common short common link and hub version 34
Figure 3.23. Semi-deployed stage of common short common link and hub version 35
Figure 3.24. Front view of folded stage of common short common link and hub version 35
Figure 3.25. Top view of folded stage of common short common link and hub version 35
Figure 3.26. Schematic diagram of dome version 36
Figure 3.27. Deployed stage of dome version 36
Figure 3.28. Semi-deployed and folded stages of dome version 36
Figure 3.29. Double layer grid unit's deployment stages (Source: Kiper, 2016) 37
Figure 3.30. Cylindrical unit's deployment stages (Source: Kiper, 2016) 37
Figure 3.31. Schematic diagram of short link to short link connection 39
Figure 3.32. Schematic diagram of long link to short link connection 39
Figure 3.33. Deployed stage of Altmann loop version 40

Figure **Page**

Figure 3.34. Semi-deployed stage of Altmann loop version 40
Figure 3.35. Folded stage of Altmann loop version 40
Figure 3.36. Schematic diagram of parallelogram loop version with long link to short link connection 41
Figure 3.37. Deployed stage of parallelogram loop version with long link to short link connection 41
Figure 3.38. Semi-deployed and folded stages of parallelogram loop version with long link to short link connection 42
Figure 3.39. Schematic diagram of short link to short link connection 42
Figure 3.40. Deployed stage of parallelogram loop version with short link to short link connection 43
Figure 3.41. Semi-deployed and folded stages of parallelogram loop version with short link to short link connection 43
Figure 3.42. Deployed stage of parallelogram loop version when links lengths are equal 43
Figure 3.43. Semi-deployed and folded stages of parallelogram loop version when links lengths are equal 44
Figure 3.44. Schematic diagram of 4-loop Altmann network 45
Figure 3.45. Deployed and semi-deployed stages of 4-loop Altmann network 45
Figure 3.46. Folded stage of 4-loop Altmann network 45

LIST OF TABLES

Table **Page**

Table 2.1. Denavit-Hartenberg parameters of the modified Altmann linkage 13
Table 2.2. Assembly Mode Angle Calculation 20

CHAPTER 1

INTRODUCTION

A mechanism is a group of rigid bodies which are connected to each other by rigid joints in order to transmit movement and force. A mechanism may contain simple and/or more complex components such as screws, wheels, cranks, belts, cams, gears, linkages, springs, and clutches (Chen 2003; Söylemez 2011).

A kinematic element is defined as the part of a rigid body that is used to connect it to a different rigid body so that the relative movement between the two rigid bodies can occur. A joint or in other words a kinematic pair is the joining of two kinematic elements. When a rigid body consists of more than two kinematic elements, a link can be obtained. Links are categorized in terms of the number of kinematic elements that they can contain, for instance binary, ternary, quaternary and so on (Söylemez 2011).

Lower kinematic pairs are the ones with surface contact, whereas higher kinematic pairs are the ones with line or point contact. A linkage is a specific type of mechanism that is composed of only lower kinematic pairs (Söylemez 2011).

Mobility analysis or determining the degree of freedom (DoF) is one of the most important stages in modelling a mechanism. Mobility is defined as the number of independent coordinates needed to identify the configuration of a mechanism (IFToMM Dictionaries Online 2014). Mobility (M) is the main parameter to affirm the existence of a mobile mechanism, to specify the number of independent parameters in modelling and also to set the input numbers required to actuate the mechanism.

There are lots of works in the literature on the mobility of mechanisms (Gogu 2005). The first works date back to the nineteenth century. Until today, several approaches and formulae were derived. In spite of the intensive literature studies, mobility calculations still remain as a main subject in the theory of mechanisms.

Among the formulae derived and presented in the literature, the most commonly used one is the one by Chebychev-Grubler-Kutzbach. According to this formulation, the mobility of a linkage can be calculated as follows (Hunt 1978):

$$m = 6(n - p - 1) + \Sigma_f \tag{1}$$

where m is the mobility of a linkage, n is the number of links, p is the number of joints, Σ_f is the sum of kinematic variables in the mechanism.

For a closed loop linkage, the loop closure equations can be obtained by multiplying transformation matrices and equating the result to an identity matrix:

$$[T_{n1}]...[T_{34}][T_{23}][T_{12}]=[I] \tag{2}$$

where $[T_{i(i+1)}]$ is the 4x4 homogeneous transformation matrix between the coordinate system of link $(i-1)i$ and the coordinate system of link $i(i+1)$, which is defined according to the Denavit-Hartenberg parameters θ_i, R_i, $\alpha_{i(i+1)}$, $a_{i(i+1)}$ presented in Figure 1.1 (Denavit and Hartenberg 1955).

$$[T_{i(i+1)}]=\begin{bmatrix} 1 & 0 & 0 & 0 \\ -a_{i(i+1)} & c\theta_i & s\theta_i & 0 \\ -R_i s\alpha_{i(i+1)} & -c\alpha_{i(i+1)}s\theta_i & c\alpha_{i(i+1)}c\theta_i & s\alpha_{i(i+1)} \\ -R_i c\alpha_{i(i+1)} & s\alpha_{i(i+1)}s\theta_i & -s\alpha_{i(i+1)}c\theta_i & c\alpha_{i(i+1)} \end{bmatrix} \tag{3}$$

where s and c are abbreviations for sine and cosine, respectively. When $i+1>n$, $i+1$ is replaced by 1.

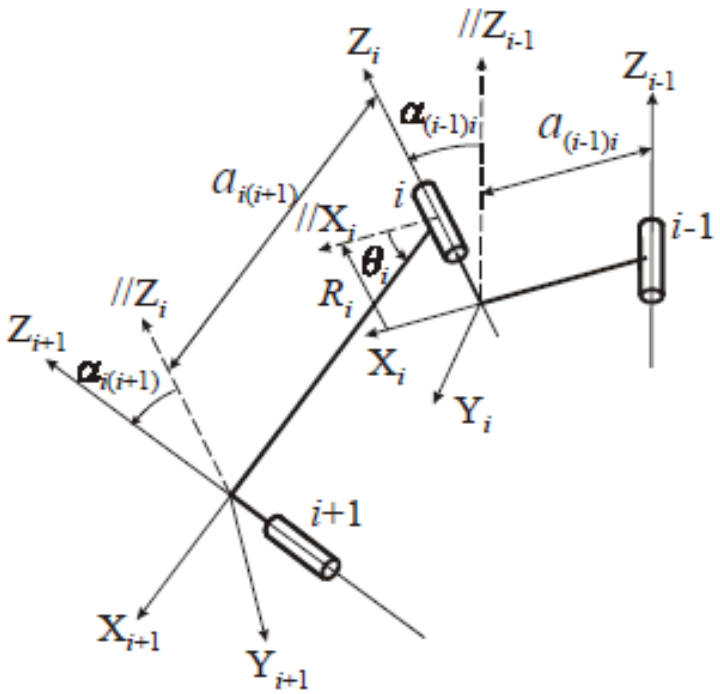

Figure 1.1 Denavit-Hartenberg patameters (Source: Chen 2003)

Note that the transformation matrix between the coordinate system of link $i(i+1)$ and the coordinate system of link $(i-1)i$ is the inverse of $\left[T_{i(i+1)}\right]$, that is

$$\left[T_{i(i+1)}\right]=\left[T_{i(i+1)}\right]^{-1}=\begin{bmatrix} 1 & 0 & 0 & 0 \\ a_{i(i+1)}c\theta_i & c\theta_i & -c\alpha_{i(i+1)}s\theta_i & s\alpha_{i(i+1)}s\theta_i \\ a_{i(i+1)}s\theta_i & s\theta_i & c\alpha_{i(i+1)}c\theta_i & -s\alpha_{i(i+1)}c\theta_i \\ -R_i & 0 & -s\alpha_{i(i+1)} & c\alpha_{i(i+1)} \end{bmatrix} \quad (4)$$

1.1. Overconstrained Linkages

There are some linkages which do not obey the Chebyshev-Grubler-Kuttzbach mobility criterion. These linkages are generally known as overconstrained linkages which means their real mobility is greater than their theoretical mobility.

Spatial overconstrained linkages are one of the types of overconstrained linkages. Philips (1984) states that the minimum number of links to construct a mobile loop with revolute joints is four. As a loop with three links and three revolute joints is either a rigid structure or an infinitesimal mechanism when all three revolute axes are coplanar and intersect at a single point. So, to construct a spatial overconstrained linkage at least four links are necessary in a mechanism.

In the following section, information about some spatial over-constrained linkages are given. The first one is the Bennett linkage (Bennett 1903) which consists 4 revolute joints and 4 links and it is a single DoF overconstrained linkage. Myard and Golberg linkages are 5R (R: revolute joint) overcontrained linkages. There are several overconstrained 6R linkages noted in the literature, but Sarrus and Altmann linkages are presented in this thesis as examples.

1.1.1. 4*R* Bennett Linkage

4R loops can be categorized according to how the joint axes are located. If all joint axes are parallel, they are called planar 4R linkages. If they all intersect at the same point, they are called as spherical 4R linkages. Any arrangement of axes other than these two

particular arrangements is generally completely rigid and therefore provides no mechanism. But there is an exception, which is the Bennett linkage (Bennett 1903).

The Bennet linkage is an exception because it is a linkage which consists of four links that have the axes of revolute joints neither concurrent, nor parallel. A Bennett linkage is illustrated in Figure 1.2. The lengths of the links are given alongside the links, and the twist angles are indicated at each joint. Bennett (1914) identified the conditions for the linkage to have a single degree of freedom.

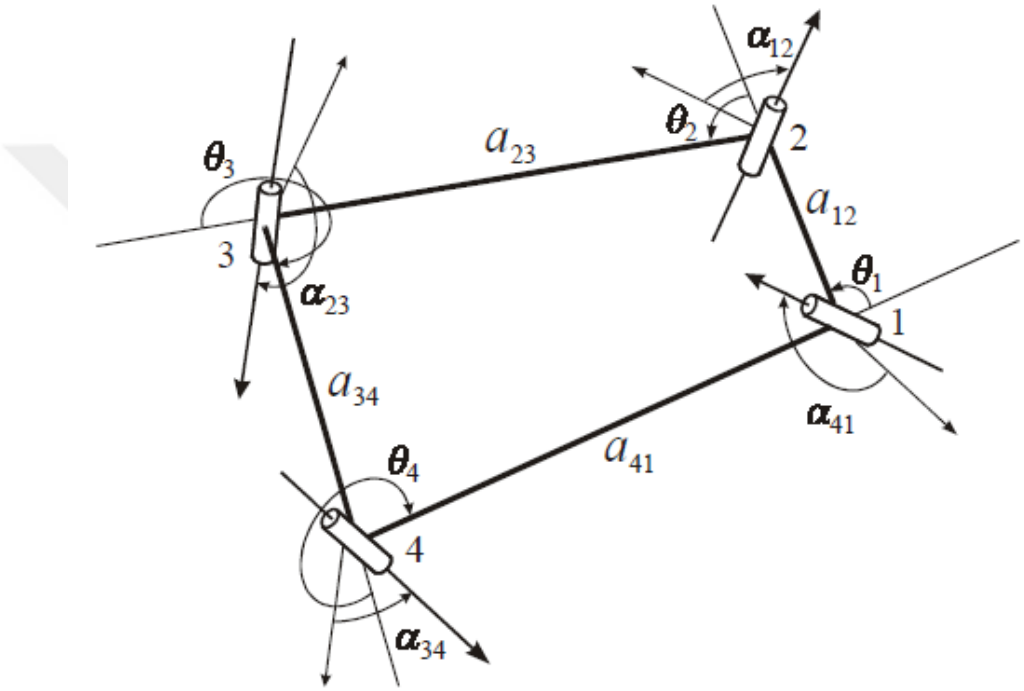

Figure 1.2. Schematic diagram of the Bennett linkage (Source: Chen, 2003)

For a Bennett linkage, two opposite links have the same length and the same twist angle:

$$a_{12} = a_{34} = a \tag{5}$$

$$a_{23} = a_{41} = b \tag{6}$$

$$\alpha_{12} = \alpha_{34} = \alpha \tag{7}$$

$$\alpha_{23} = \alpha_{41} = \beta \tag{8}$$

Furthermore, the link lengths and twist angles should satisfy the following condition:

$$\frac{\sin\alpha}{a} = \frac{\sin\beta}{b} \tag{9}$$

Joint offsets are all zero:

$$R_i = 0 \quad (i = 1, 2, 3, 4) \tag{10}$$

The values of the revolute joint variables, θ_1, θ_2, θ_3 and θ_4, vary when the linkage moves according to

$$\begin{aligned} \theta_1 + \theta_3 &= 2\pi \\ \theta_2 + \theta_4 &= 2\pi \end{aligned} \tag{11}$$

and

$$\tan\frac{\theta_1}{2}\tan\frac{\theta_2}{2} = \frac{\sin\frac{1}{2}(\alpha_{23} + \alpha_{12})}{\sin\frac{1}{2}(\alpha_{23} - \alpha_{12})} \tag{12}$$

These three closure equations ensure that only one of the joint angles is independent, so the linkage has a single degree of Freedom (Baker 1978). Bennett (1914) also identified some special cases:

(a) An equilateral linkage is obtained if $\alpha + \beta = \pi$ and $a = b$. Eq. (12) then becomes

$$\tan\frac{\theta_1}{2}\tan\frac{\theta_2}{2} = \frac{1}{\cos\alpha} \tag{13}$$

(b) If $\alpha = \beta$ and $a = b$, the four links are congruent. The motion is discontinuous: $\theta_1 = \pi$ allows any value for θ_2 and $\theta_2 = \pi$ allows any value for θ_1.

(c) If $\alpha = \beta = 0$, the linkage is a planar crossed parallelogram linkage.

(d) If $\alpha = 0$ and $\beta = \pi$, the linkage becomes a planar parallelogram linkage.

(e) If $a = b = 0$, the linkage is a spherical 4*R* linkage (Phillips 1990).

Since the Bennett linkage consists of minimum number of links, a lot of studies have been conducted on it. Most of these studies focus on the mathematical representation and the kinematic analysis of the linkage. There are some studies based on building 5R or 6R spatial linkages using the Bennett linkage. In the next sub-section, information about some of these linkages are given. Baker and Hu tried to connect two Bennett linkages, but it was an unsuccessful attempt (Baker and Hu 1986). Chen (2003) provided several deployable networks comprising Bennett loops, where adjacent loops are connected to each other with two additional revolute joints. Isaak (2006), Kiper and Söylemez (2009), Tian and Chen (2010), Guo and You (2012), Yang et al. (2015) also presented some assemblies of Bennett linkages.

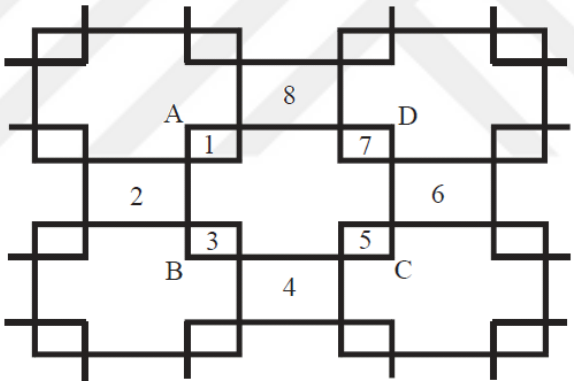

Figure 1.3. Bennet Network of Chen (Source: Chen 2003)

1.1.2. 5*R* Linkages

Goldberg (1943) and Myard (1931) linkages are the 5R linkages reported in the literature. A Goldberg 5R linkage is actually combination of a pair of Bennett linkages. This combination can be obtained by removing a link common to both of the Bennett linkages and by rigidly attaching a pair of adjacent links to each other. The method developed by Goldberg can be summarized as addition of two Bennett loops in order to obtain a 5R linkage, as shown in Figure 1.4 (Goldberg 1943).

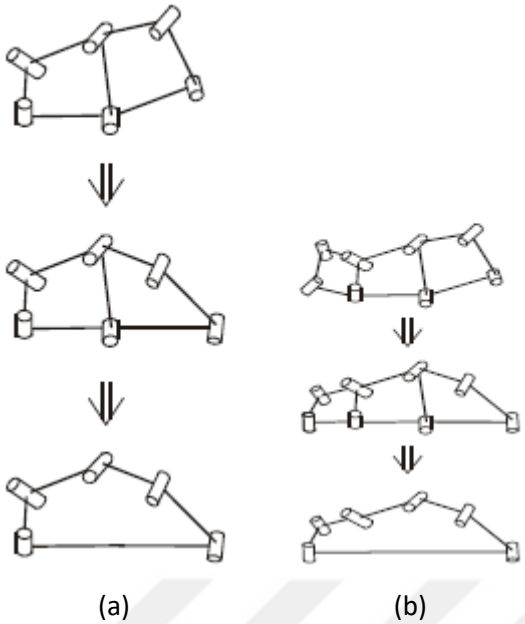

Figure 1.4. Goldberg (a) 5R Linkage, (b) 6R Linkage (Source: Goldberg 1943)

Before Goldberg, Myard (1931) developed an overconstrained 5R linkage which is shown in Figure 1.5. This linkage has later been re-categorized as a particular case of the Goldberg 5R linkage.

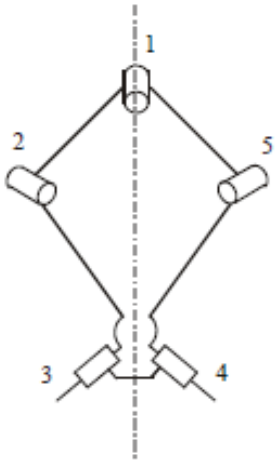

Figure 1.5. Myard linkage (Source: Kiper 2018)

Myard linkage is constructed by combining two mirror-symmetrical Bennett 4R loops with two common links and common joints in mirror symmetrical position and removing the common links and one of the common joints (Baker 1979).The conditions on its Denavit-Hartenberg parameters are as follows:

$$a_{34} = 0,\ a_{12} = a_{51},\ a_{23} = a_{45}$$
$$\alpha_{23} = \alpha_{45} = \frac{\pi}{2},\ \alpha_{51} = \pi - \alpha_{12},\ \alpha_{34} = \pi - 2\alpha_{12} \quad (14)$$
$$R_1 = R_2 = R_3 = R_4 = R_5 = 0$$

Myard linkage has been used as a module in deployable structures by Briand and You Z (2007), Liu and Chen (2009), Qi et al. (2011).

1.1.3. 6*R* Linkages

Many 6R linkages are presented in the literature. In the following subsections, information about two of them, Sarrus and Altmman linkages, is given.

1.1.3.1. Sarrus Linkage

The first published spatial overconstrained linkage is the Sarrus linkage (Sarrus 1853). Bennett (1905) built a model of this linkage as presented in Figure 1.6(a), along with a schematic chart in Figure 1.6(b). The A, R, S, and B links are consequentially combined by three parallel horizontal joints, as also the A, T, U and B links are. These two sets of joints are different from each other in terms of their directions. According to this arrangement A link can move vertically up and down with respect to B link.

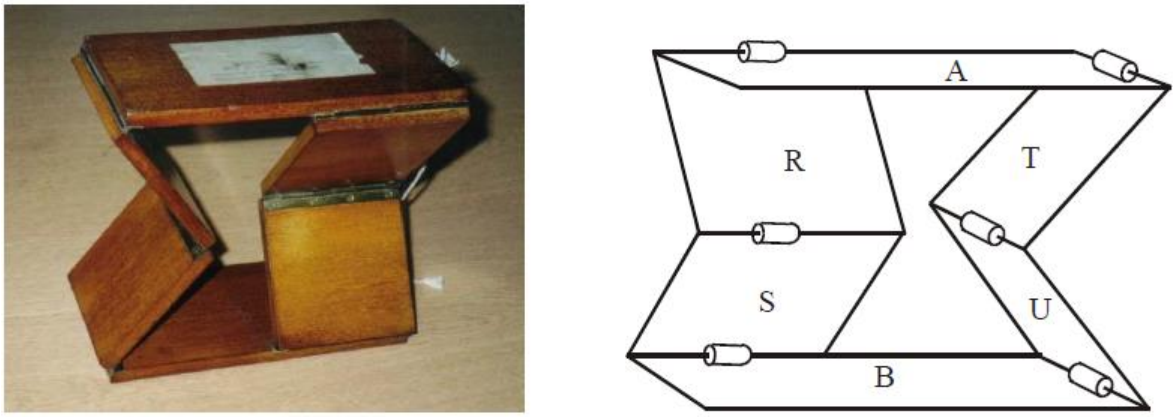

(a) (b)

Figure 1.6. Sarrus linkage, (a) Bennet's Model, (b) schematic diagram (Source: Chen 2003)

In deployable structures, the Sarrus linkage frequently appears as a connecting loop when two or more planar scissor linkages in different planes are to be connected to each other. Kiper and Söylemez (2010) and Bouten (2015) have presented some assemblies of Sarrus loops as deployable structures.

1.1.3.2. Altmann Linkage

Altmann (1954) introduced a 6*R* linkage as presented in Figure 1.7, which is a special case of a Bricard line-symmetric linkage. The dimensional conditions of the linkage can be listed as follows:

$$\begin{aligned} &a_{12} = a_{45} = a,\ a_{23} = a_{56} = 0,\ a_{34} = a_{61} = b \\ &\alpha_{12} = \alpha_{45} = \frac{\pi}{2},\ \alpha_{23} = \alpha_{56} = \frac{\pi}{2},\ \alpha_{34} = \alpha_{61} = \frac{3\pi}{2} \\ &R_i = 0 \quad (i = 1,\ 2,\ ...,\ 6) \end{aligned} \tag{15}$$

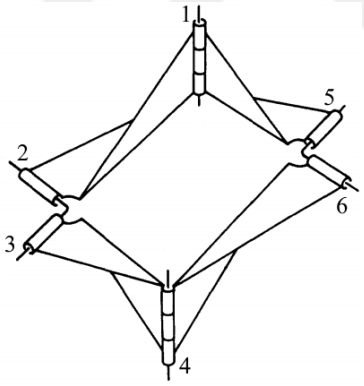

Figure 1.7. Altmann linkage (modified from (Baker, 1993))

The pair of joints 2-3 and 5-6 are perpendicularly intersecting each other, hence they can be considered as universal (U) joints. In this perspective, the Altmann linkage can be considered as a line-symmetric RURU linkage.

In the literature, there are only a few number of studies related with the analysis of the Altmann linkage. Baker (1993) intended to algebraically analyze the Altmann linkage in order to obtain a direct solution. By using screw algebra, the specific configurations, angular velocities and relative motion is investigated. Song et al. (2016) worked on the feasibility of the constructing of a large deployable network by using

Altmann linkages. Using Altmann linkages as modules, they constructed deployable networks with the overlapping-unit method under appropriate connections (Figure 1.8).

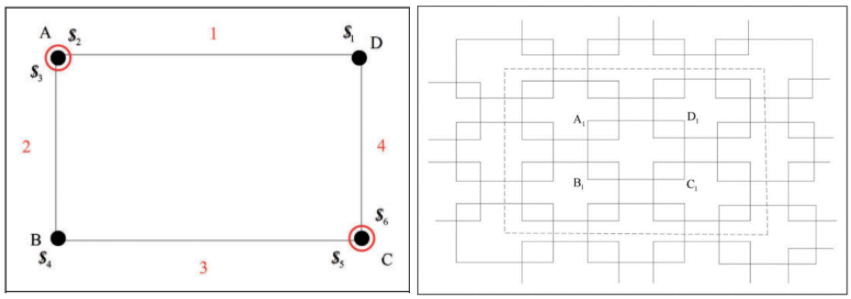

(a) (b)

Figure 1.8.(a) Schematic of an Altmann Linkage, (b) A deployable network constructed by Altmann linkages (Source: Song et al. 2016)

Atarer et al. (2017) studied on the design alternatives of network constructed by Altmann linkages. In the study, the authors focused on a modified version (Figure 1.9) of the Altmann linkage and they investigated the possibility of building network of single DoF deployable structures by using modified Altmann linkages as modules. In addition to that, they focused on the probability of assembly alternatives with only revolute joints. Two alternative ways of connections to build the network are proposed: with common links and joints and with new joints. By using common links and joints, they obtained three different networks of Altmann linkages: the scissor, arch and dome versions. By using new joints, they obtained two different networks of Altmann linkages: the Altmann loop and parallelogram loop versions. These assemblies are evaluated in detail in Chapter 3.

Figure 1.9. Model of a modified Altmann linkage (Source: Atarer, Korkmaz, and Kiper 2017)

1.2. Aim and Scope

A modified version of the Altmann linkage is proposed in (Atarer, Korkmaz, and Kiper 2017) , but there is no study related with the kinematic analysis of this linkage in the literature. His study is intended to perform modelling and analyzing of modified version of Altmann linkage. Within the scope of the study, modified Altmann linkage is described, kinematic analysis of the linkage is derived in Chapter 2. Possible networks comprising modified Altmann linkages are obtained in Chapter 3. Conclusions are presented in Chapter 4.

CHAPTER 2

MODIFIED ALTMANN LINKAGE

In the original Altmann linkage, all joint offsets are zero (Figure 1.7) and this complicates the constructional design of a real model. As a solution for this complication, the modified Altmann linkage is proposed in (Atarer, Korkmaz, and Kiper 2017) such that four of the joint offsets are nonzero. Thanks to these nonzero joint offsets (d), it is possible to introduce two links with square cross-section at the U joints as depicted in Figure 2.1.

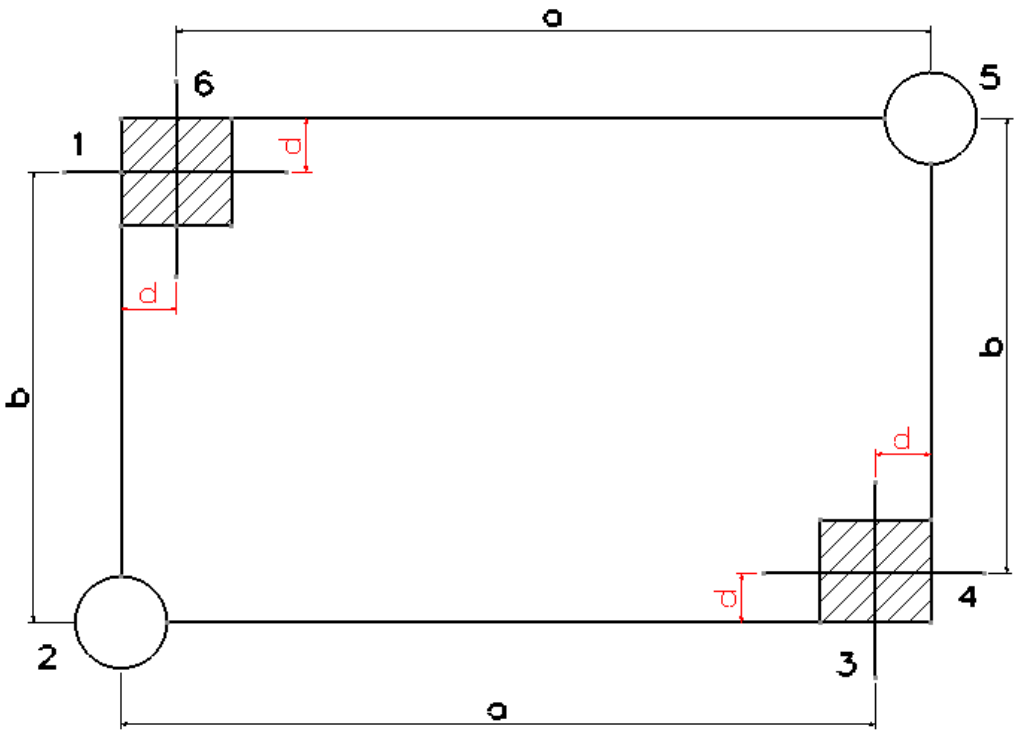

Figure 2.1. Schematic representation of the modified Altmann linkage

The Denavit-Hartenberg parameters to represent relative positions of joint axes and links of a linkage are

- θ_i: measured about z_i-axis from x_{i-1}-axis to x_i-axis according to right hand rule

- d_i: measured along z_i-axis from x_{i-1}-axis to x_i-axis ($|d_i|$ = shortest distance from x_{i-1}-axis to x_i-axis; d_i may be negative)
- α_{ij}: measured about x_i-axis from z_i-axis to z_j-axis (j = i + 1) according to right hand rule
- a_{ij}: shortest distance (always nonnegative) between z_i-axis and z_j-axis

z_i-axes are positioned along the joint axes and x_i-axes are positioned along the common perpendiculars between consecutive joint axes (Figure 2.2). In Table 2.1, the Denavit-Hartenberg parameters for the modified Altmann linkage are listed.

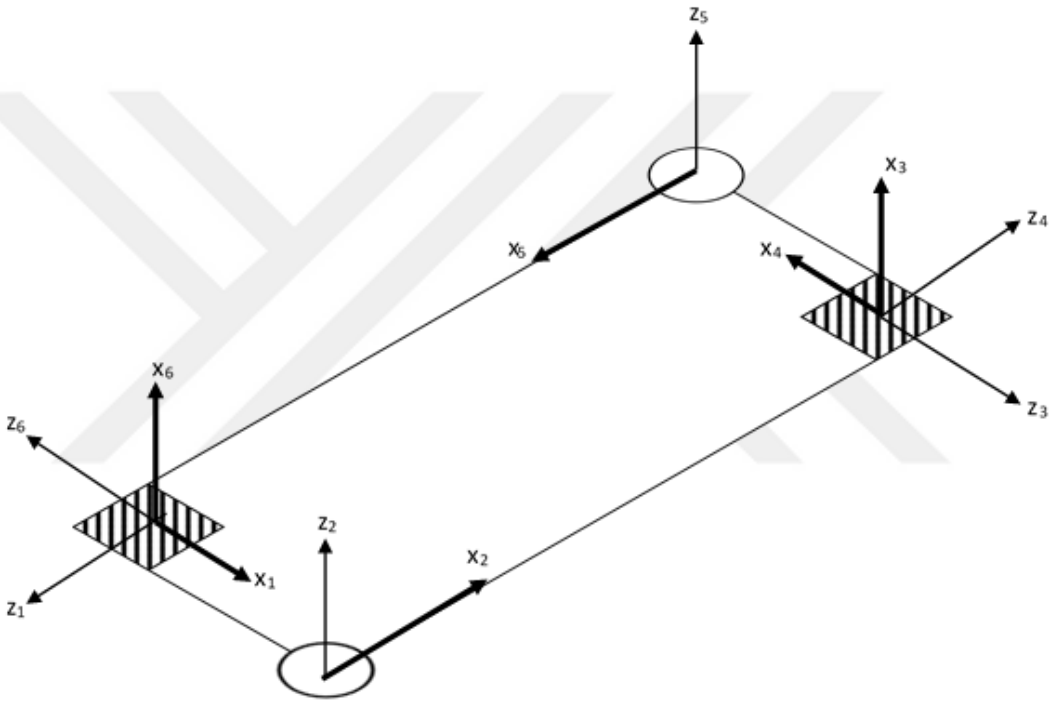

Figure 2.2. Attached reference frames to the modified Altmann linkage

Table 2.1. Denavit-Hartenberg parameters of the modified Altmann linkage

Frame	θ_i	d_i	a_{ij}	α_{ij}
1	θ_1	d	b	$3\pi/2$
2	θ_2	0	a	$\pi/2$
3	θ_3	-d	0	$\pi/2$
4	θ_4	d	b	$3\pi/2$
5	θ_5	0	a	$\pi/2$
6	θ_6	-d	0	$\pi/2$

The following transformation matrices are used for writing the loop closure equations:

$$X = \begin{bmatrix} 1 & 0 & 0 & a_{ij} \\ 0 & \cos\alpha_{ij} & -\sin\alpha_{ij} & 0 \\ 0 & \sin\alpha_{ij} & \cos\alpha_{ij} & 0 \\ 0 & 0 & 0 & 1 \end{bmatrix} \quad Z = \begin{bmatrix} \cos\theta_{ij} & -\sin\theta_{ij} & 0 & 0 \\ \sin\theta_{ij} & \cos\theta_{ij} & 0 & 0 \\ 0 & 0 & 1 & d_{ij} \\ 0 & 0 & 0 & 1 \end{bmatrix} \tag{16}$$

The loop closure equations read ([I] is a 4x4 identity matrix).

$$[Z(\theta_1, d_1)][X(\alpha_{12}, a_{12})][Z(\theta_2, d_2)]\ldots[X(\alpha_{56}, a_{56})][Z(\theta_6, d_6)][X(\alpha_{61}, a_{61})] = [I] \tag{17}$$

In order to verify Eq.(17), a 3D model of the modified Altmann linkage is modeled in a CAD program and the joint angles are measured as depicted in Figure 2.3.

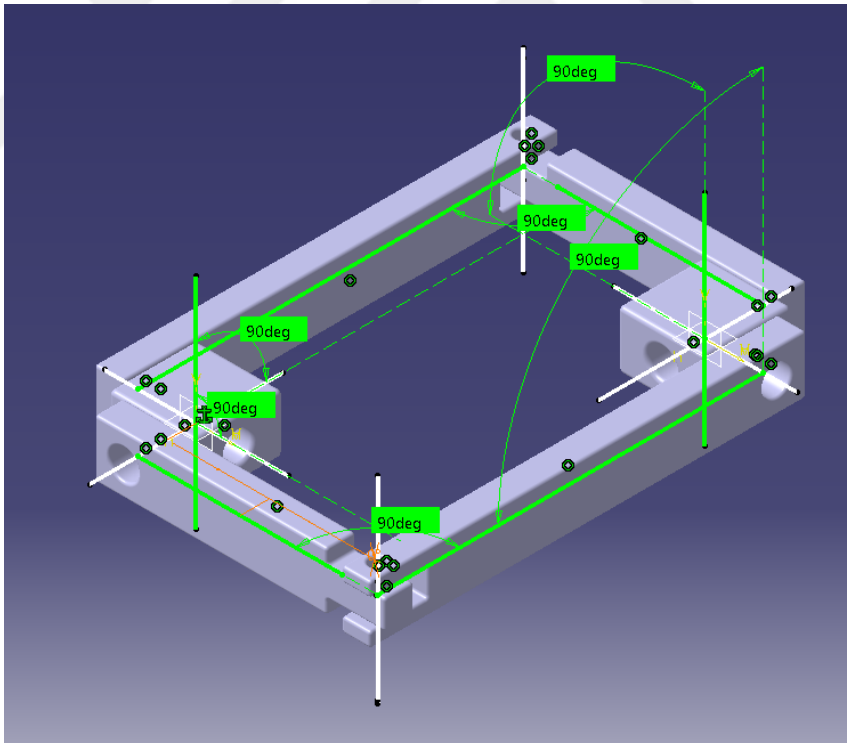

Figure 2.3. Modified Altmann linkage

The link lengths used in the CAD model are as follows: a = 265, b = 165, d = 10. The joint angle values measured from the CAD model are as follows: $\theta_2 = \theta_3 = \theta_5 = \theta_6 = \pi/2$, $\theta_1 = \theta_4 = -\pi/2$.

4x4 homogeneous transformation matrix calculation for the modified Altmann linkage with given parameters is as follows:

$$[D]=[Z(\frac{3\pi}{2},40)][X(\frac{3\pi}{2},165)][Z(\frac{\pi}{2},0)][X(\frac{\pi}{2},265)][Z(\frac{\pi}{2},-40)][X(\frac{\pi}{2},0)]\cdots$$
$$\cdots[Z(\frac{3\pi}{2},40)][X(\frac{3\pi}{2},165)][Z(\frac{\pi}{2},0)][X(\frac{\pi}{2},265)][Z(\frac{\pi}{2},-40)][X(\frac{\pi}{2},0)] \quad (18)$$

When the matrices in Eq. (18) are written in full form and the multiplications are performed, it is seen that the matrix [D] is a 4x4 identity matrix. Eq. (17) has been verified with different set of joint angle values as well.

For the kinematic analysis of a general modified Altmann linkage:

$$[I]=[Z(\theta_1,d)][X(\frac{3\pi}{2},b)][Z(\theta_2,0)][X(\frac{\pi}{2},a)][Z(\theta_3,-d)][X(\frac{\pi}{2},0)]\cdots$$
$$\cdots[Z(\theta_4,d)][X(\frac{3\pi}{2},b)][Z(\theta_5,0)][X(\frac{\pi}{2},a)][Z(\theta_6,-d)][X(\frac{\pi}{2},0)] \quad (19)$$

Post-multiplying Eq. (19) with the inverse of the multiplication of the last nine matrices:

$$[X(-\frac{\pi}{2},0)][Z(-\theta_6,d)][X(-\frac{\pi}{2},-a)][Z(-\theta_5,0)][X(-\frac{3\pi}{2},-b)][Z(-\theta_4,-d)]\cdots$$
$$\cdots[X(-\frac{\pi}{2},0)][Z(-\theta_3,d)][X(-\frac{\pi}{2},-a)]=[Z(\theta_1,d)][X(\frac{3\pi}{2},b)][Z(\theta_2,0)] \quad (20)$$

Writing all matricies in full form in Eq. (20):

$$\begin{bmatrix}1&0&0&0\\0&0&1&0\\0&-1&0&0\\0&0&0&1\end{bmatrix}\begin{bmatrix}c_6&s_6&0&0\\-s_6&c_6&0&0\\0&0&1&d\\0&0&0&1\end{bmatrix}\begin{bmatrix}1&0&0&-a\\0&0&1&0\\0&-1&0&0\\0&0&0&1\end{bmatrix}\begin{bmatrix}c_5&s_5&0&0\\-s_5&c_5&0&0\\0&0&1&0\\0&0&0&1\end{bmatrix}\begin{bmatrix}1&0&0&-b\\0&0&-1&0\\0&1&0&0\\0&0&0&1\end{bmatrix}\begin{bmatrix}c_4&s_4&0&0\\-s_4&c_4&0&0\\0&0&1&-d\\0&0&0&1\end{bmatrix}$$
$$\begin{bmatrix}1&0&0&0\\0&0&1&0\\0&-1&0&0\\0&0&0&1\end{bmatrix}\begin{bmatrix}c_3&s_3&0&0\\-s_3&c_3&0&0\\0&0&1&d\\0&0&0&1\end{bmatrix}\begin{bmatrix}1&0&0&-a\\0&0&1&0\\0&-1&0&0\\0&0&0&1\end{bmatrix}=\begin{bmatrix}c_1&-s_1&0&0\\s_1&c_1&0&0\\0&0&1&d\\0&0&0&1\end{bmatrix}\begin{bmatrix}1&0&0&b\\0&0&1&0\\0&-1&0&0\\0&0&0&1\end{bmatrix}\begin{bmatrix}c_2&-s_2&0&0\\s_2&c_2&0&0\\0&0&1&0\\0&0&0&1\end{bmatrix} \quad (21)$$

where c_i and s_i are abbreviations for cosine(θ_i) and sine(θ_i), respectively for i = 1, …, 6. Performing the matrix multiplications:

$$\begin{bmatrix} (c_4c_5c_6 - s_4s_6)c_3 - s_3s_5c_6 & -s_4c_5c_6 - c_4s_6 & (c_4c_5c_6 - s_4s_6)s_3 + c_3s_5c_6 & t_x \\ c_3c_4s_5 - s_3c_5 & -s_4s_5 & s_3c_4s_5 - c_3c_5 & t_y \\ (c_4c_5s_6 + s_4c_6)c_3 - s_3s_5s_6 & -s_4c_5s_6 + c_4c_6 & (c_4c_5s_6 + s_4c_6)s_3 + c_3s_5s_6 & t_z \\ 0 & 0 & 0 & 1 \end{bmatrix} = \begin{bmatrix} c_1c_2 & -c_1s_2 & -s_1 & c_1b \\ s_1c_2 & -s_1s_2 & c_1 & s_1b \\ -s_2 & -c_2 & 0 & d \\ 0 & 0 & 0 & 1 \end{bmatrix} \quad (22)$$

where $t_x = -\left[(c_4c_5c_6 - s_4s_6)c_3 - s_3s_5c_6\right]a + (s_4c_5c_6 + c_4s_6)d + s_5c_6d - c_5c_6b - c_6a$,
$t_y = -(c_3c_4s_5 + s_3c_5)a + s_4s_5d - c_5d - s_5b + d$ and
$t_z = -\left[(c_4c_5s_6 + s_4c_6)c_3 - s_3s_5s_6\right]a + (s_4c_5c_6 - c_4c_6)d + s_5s_6d - c_5s_6b - s_6a$.

Equating the rightmost columns of Eq. (22):

$$c_1b = -\left[(c_4c_5c_6 - s_4s_6)c_3 - s_3s_5c_6\right]a + (s_4c_5c_6 + c_4s_6)d + s_5c_6d - c_5c_6b - c_6a \quad (23)$$

$$s_1b = -(c_3c_4s_5 + s_3c_5)a + s_4s_5d - c_5d - s_5b + d \quad (24)$$

$$d = -\left[(c_4c_5s_6 + s_4c_6)c_3 - s_3s_5s_6\right]a + (s_4c_5c_6 - c_4c_6)d + s_5s_6d - c_5s_6b - s_6a \quad (25)$$

Rearranging Eqs. (23)-(25):

$$c_1(b + c_2a - s_2d) = c_6(s_5d - c_5b - a) \quad (26)$$

$$s_1(b + c_2a - s_2d) = -(c_5d + s_5b - d) \quad (27)$$

$$(d - s_2a - c_2d) = s_6(s_5d - c_5b - a) \quad (28)$$

Taking squares and summing Eq. (26)-(28) results as following:

$$c_2\left(ab-d^2\right)-s_2\left(db-ad\right)=c_5\left(ab-d^2\right)-s_5\left(db-ad\right) \tag{29}$$

$c_2 = c_5$ and $s_2 = s_5$ implies that $\theta_5 = \theta_2$. Equating the second row and second column elements of Eq. (22) shows that $s_1 = s_4$, so $\theta_4 = \theta_1$. Equating (3,1) and (3,3) elements of the rotation matrix and using equalities given above:

$$\begin{aligned}\left(c_1c_2s_6+s_1c_6\right)c_3-s_2s_3s_6&=-s_2\\ \left(c_1c_2s_6+s_1c_6\right)s_3+s_2c_3s_6&=0\end{aligned} \tag{30}$$

Rearranging Eq. (30):

$$\begin{bmatrix}c_3 & -s_3\\ s_3 & c_3\end{bmatrix}\begin{bmatrix}c_1c_2s_6+s_1c_6\\ s_2s_6\end{bmatrix}=\begin{bmatrix}-s_2\\ 0\end{bmatrix}\Rightarrow$$
$$\begin{bmatrix}c_1c_2s_6+s_1c_6\\ s_2s_6\end{bmatrix}=\begin{bmatrix}c_3 & s_3\\ -s_3 & c_3\end{bmatrix}\begin{bmatrix}-s_2\\ 0\end{bmatrix}=\begin{bmatrix}-c_3s_2\\ s_2s_3\end{bmatrix} \tag{31}$$

From the last row of Eq. (31), $s_3 = s_6$. Equating (1,1), (1,3) elements of the rotation matrix and using equalities given above:

$$\begin{aligned}\left(c_1c_2c_6-s_1s_6\right)c_3-s_2c_6s_3&=c_1c_2\\ \left(c_1c_2c_6-s_1s_6\right)s_3+s_2c_6c_3&=-s_1\end{aligned} \tag{32}$$

Rearranging Eq. (32):

$$\begin{bmatrix}c_3 & -s_3\\ s_3 & c_3\end{bmatrix}\begin{bmatrix}c_1c_2c_6-s_1s_6\\ s_2c_6\end{bmatrix}=\begin{bmatrix}c_1c_2\\ -s_1\end{bmatrix}\Rightarrow$$
$$\begin{bmatrix}c_1c_2c_6-s_1s_6\\ s_2c_6\end{bmatrix}=\begin{bmatrix}c_3 & s_3\\ -s_3 & c_3\end{bmatrix}\begin{bmatrix}c_1c_2\\ -s_1\end{bmatrix}=\begin{bmatrix}c_1c_2c_3-s_1s_3\\ -c_1c_2s_3-s_1c_3\end{bmatrix} \tag{33}$$

From the last row of Eq. (33), $c_3 = c_6$. Therefore, $\theta_6 = \theta_3$. Rewriting Eq. (22):

$$\begin{bmatrix} (c_1c_2c_3 - s_1s_3)c_3 - s_2c_3s_3 & -s_1c_2c_3 - c_1s_3 & (c_1c_2c_3 - s_1s_3)s_3 + s_2c_3^2 & t_x \\ c_1s_2c_3 + c_2s_3 & -s_1s_2 & c_1s_2s_3 - c_2c_3 & t_y \\ (c_1c_2s_3 + s_1c_3)c_3 - s_2s_3^2 & -s_1c_2s_3 + c_1c_3 & (c_1c_2s_3 + s_1c_3)s_3 + s_2s_3c_3 & t_z \\ 0 & 0 & 0 & 1 \end{bmatrix} = \begin{bmatrix} c_1c_2 & -c_1s_2 & -s_1 & c_1b \\ s_1c_2 & -s_1s_2 & c_1 & s_1b \\ -s_2 & -c_2 & 0 & d \\ 0 & 0 & 0 & 1 \end{bmatrix} \tag{34}$$

Equating (1,1), (1,2), (2,1), (3,1), (3,2) elements of the rotation matrix:

$$\begin{aligned} &(c_1c_2c_3 - s_1s_3)c_3 - s_2c_3s_3 = c_1c_2 \\ &s_1c_2c_3 + c_1s_3 = c_1s_2 \\ &c_1s_2c_3 + c_2s_3 = s_1c_2 \\ &(c_1c_2s_3 + s_1c_3)c_3 - s_2s_3^2 = -s_2 \\ &s_1c_2s_3 - c_1c_3 = c_2 \end{aligned} \tag{35}$$

Equating the rightmost columns of Eq. (34):

$$c_1b = -\left[(c_1c_2c_3 - s_1s_3)c_3 - s_3s_2c_3\right]a + (s_1c_2c_3 + c_1s_3)d + s_2c_3d - c_2c_3b - c_3a \tag{36}$$

$$s_1b = -(c_3c_1s_2 + s_3c_2)a + s_1s_2d - c_2d - s_2b + d \tag{37}$$

$$d = -\left[(c_1c_2s_3 + s_1c_3)c_3 - s_2s_3^2\right]a + (s_1c_2c_3 - c_1c_3)d + s_2s_3d - c_2s_3b - s_3a \tag{38}$$

Substituting Eq. (35) in Eqs. (36)-(38):

$$c_1(b + c_2a - s_2d) = c_3(s_2d - c_2b - a) \tag{39}$$

$$s_1(b + c_2a - s_2d) = -s_2b + (1 - c_2)d \tag{40}$$

$$-s_2a + (1 - c_2)d = s_3(s_2d - c_2b - a) \tag{41}$$

Using Eq. (40) with a given input angle θ_2, θ_1 can be found from

$$s_1 = \frac{-s_2 b + (1 - c_2) d}{b + c_2 a - s_2 d} \tag{42}$$

Using Eq. (41) with a given input angle θ_2, θ_3 can be found from

$$s_3 = \frac{s_2 a + (c_2 - 1) d}{a + c_2 b - s_2 d} \tag{43}$$

For a = b Eqs. (42)-(43) become

$$s_1 = -\tan\frac{\theta_2}{2} \quad \text{and} \quad s_3 = \tan\frac{\theta_2}{2} \tag{44}$$

This means that when a = b, the relationship between the joint angles does not depend on any link lengths. All equilateral linkages (a = b) have the same behavior no matter what d is. Eq. (44) also holds for an Altmann linkage (d = 0) with equal link lengths (a = b). Furthermore, $\theta_3 = \theta_1 + \pi$ when a = b.

Since $\sin(\beta) = \sin(\pi - \beta)$, there are two different assembly modes of the modified Altmann linkage, which is illustrated in Figure 2.4.

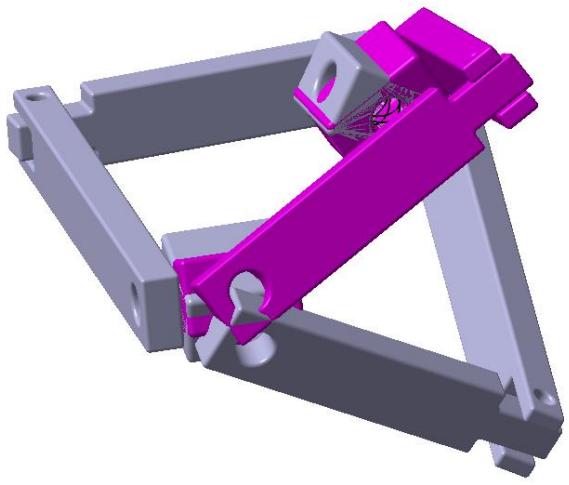

Figure 2.4. Assembly modes of a modified Altmann linkage

A simple calculation can be done to verify these two modes of the modified Altmann linkage. Using the link lengths a = 265, b = 165, d = 40, Eqs. (42)-(43) with a given input angle of θ_2, the joint angle values listed in Table 2.2 can be obtained. These calculated values are verified with a CAD model (Figure 2.5).

Table 2.2. Assembly Mode Angle Calculation

θ_2 (deg)	θ_2 (rad)	θ_1 (deg)	θ_1 (rad)	θ_3 (deg)	θ_3 (rad)
85	1.48353	-59.5939	-1.04011	108.2549	1.252189
		-120.406		71.74513	

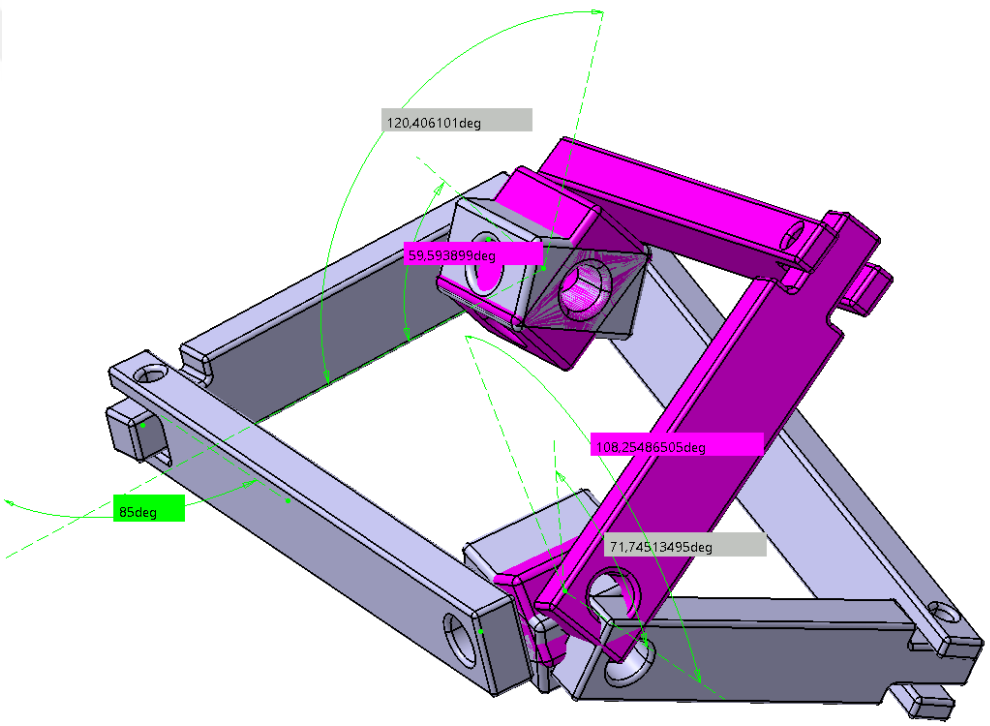

Figure 2.5. Output angle verification of assembly modes of a modified Altmann linkage

Further study has been done to find the relationship between input and output angles for different link length proportions. 3 different link length ratios (a/b) and 3 different joint offset values (d) are used during the examination. Link length ratios are taken as, $a = b$, $a = 1.5b$ and $a = 2b$. Joint offset values are taken as $d = a/10$, $d = 2a/10$ and $d = 4a/10$.

1. $a = b$ case: For this case, it is numerically verified that the input/output relationship does not depend on link lengths and that $\theta_1 = \theta_3 + \pi$ (Figure 2.6-2.7).

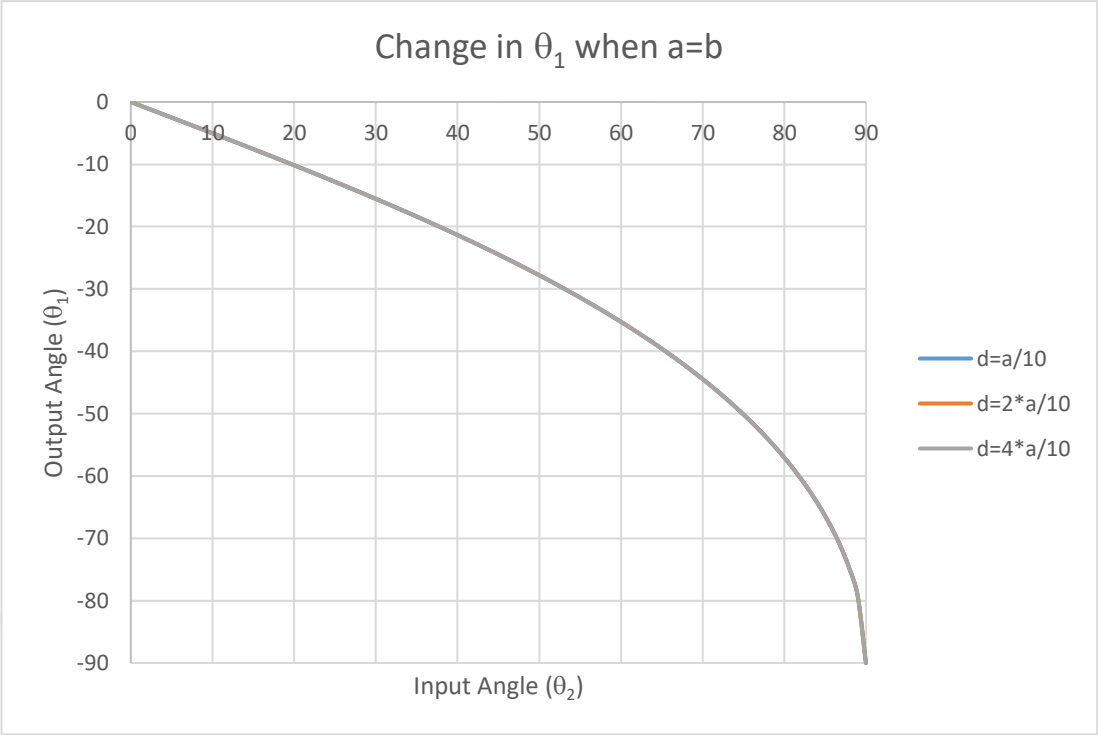

Figure 2.6. Input (θ_2)/output (θ_1) relationship when $a = b$

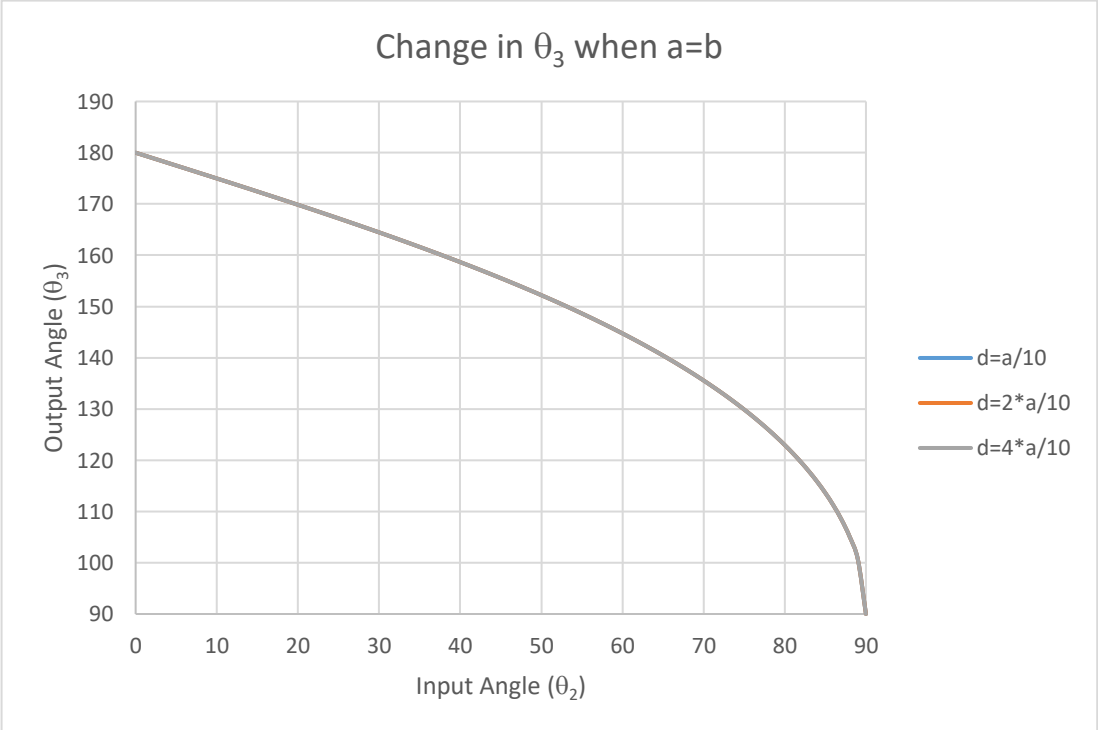

Figure 2.7. Input (θ_2)/output (θ_3) relationship when $a = b$

2. $a = 1.5b$ case: As it can be seen from Figure 2.8-Figure 2.9, change of the joint offset value slightly affects the output angle in this case.

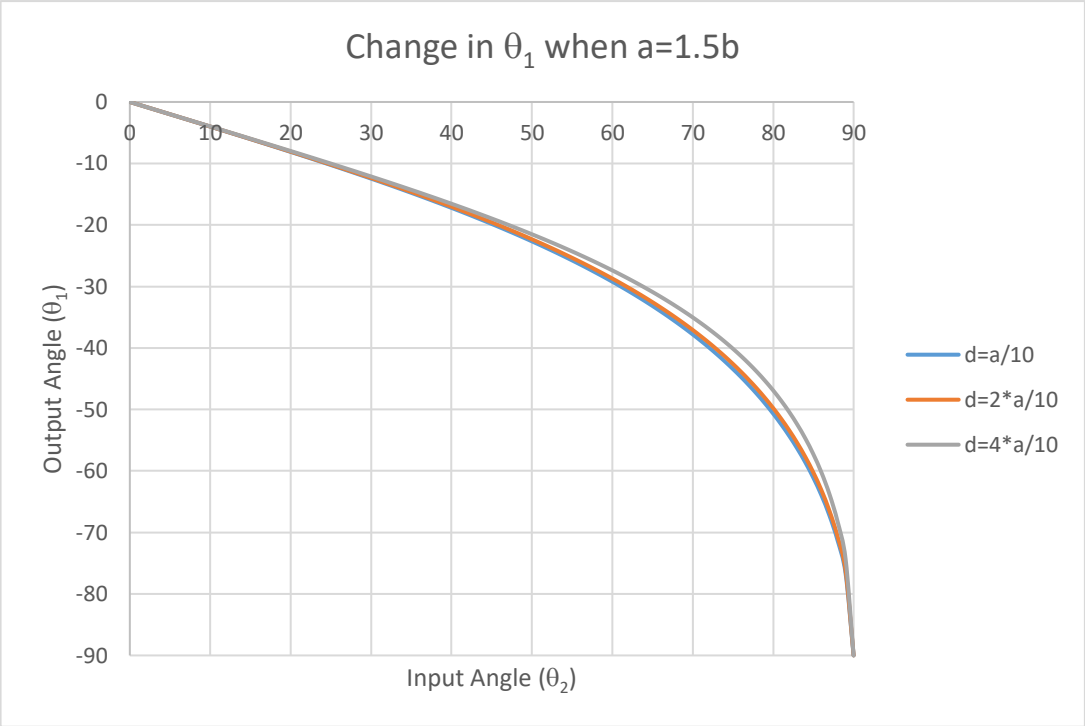

Figure 2.8. Input (θ_2)/output (θ_1) relationship when $a = 1.5b$

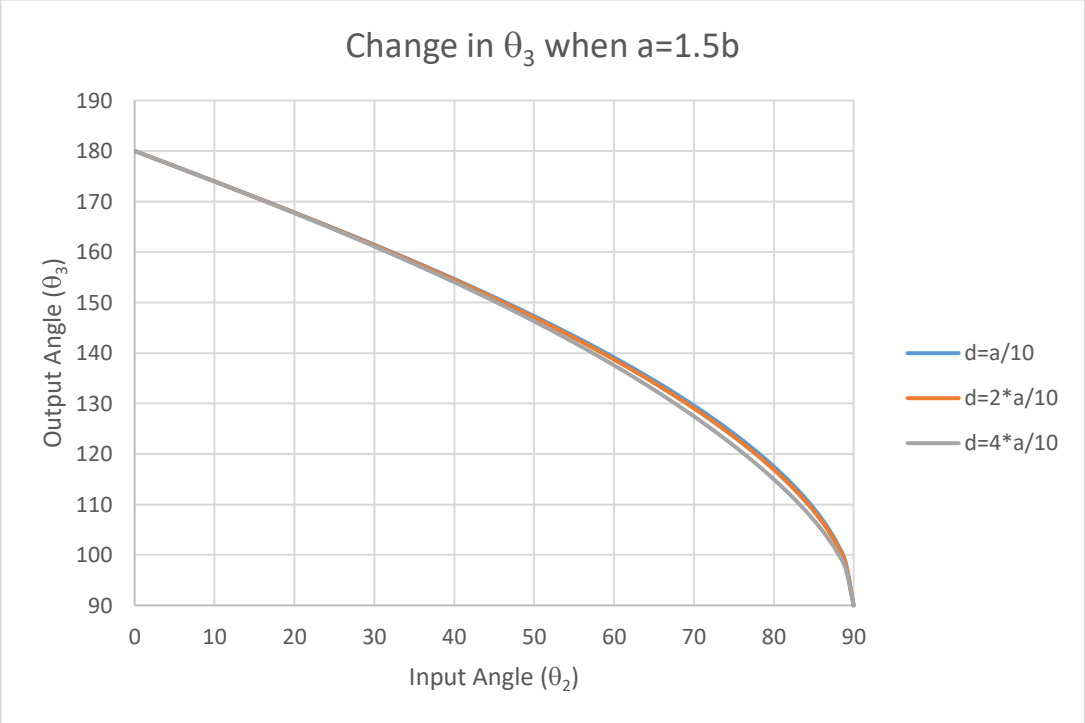

Figure 2.9. Input (θ_2)/output (θ_3) relationship when $a = 1.5b$

3. $a = 2b$ case: As it can be seen from Figure 2.10-Figure 2.11, change of the joint offset value slightly affects the output angle in this case, but the difference is more compared to the $a = 1.5b$ case.

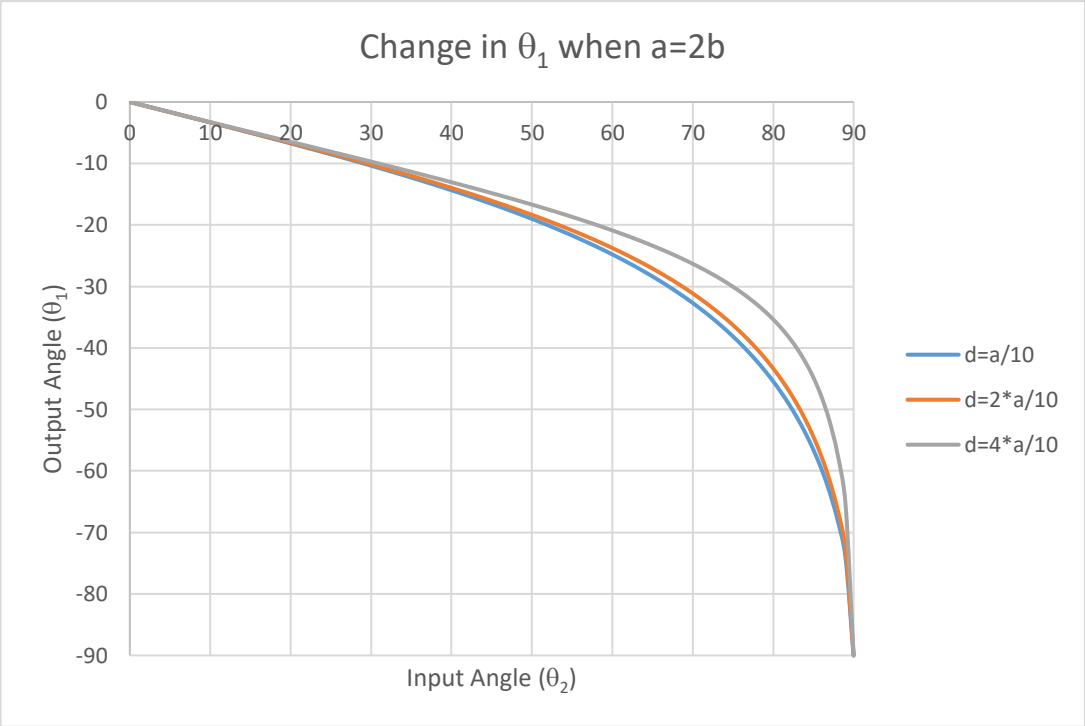

Figure 2.10. Input (θ_2)/output (θ_1) relationship when $a = 2b$

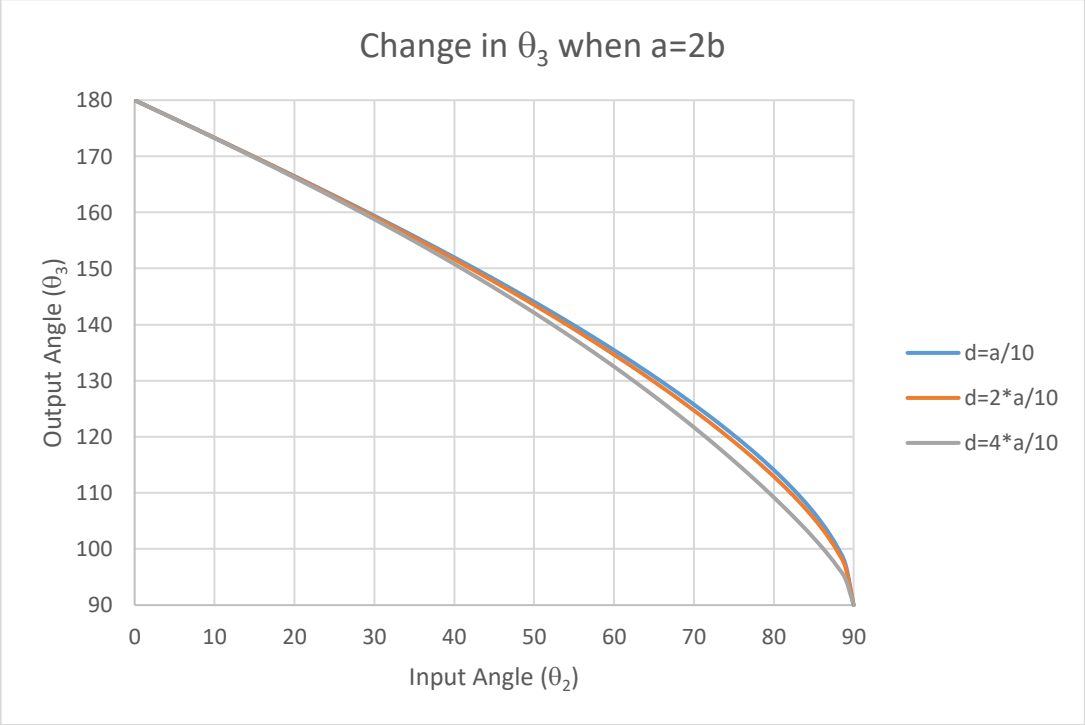

Figure 2.11. Input (θ_2)/output (θ_3) relationship when $a = 2b$

CHAPTER 3

DEPLOYABLE STRUCTURES COMPRISING MODIFIED ALTMANN LINKAGES

Most deployable structures are assemblies or networks of certain basic elements. Obtaining new deployable networks by connecting equivalent or similar copies of a selected single-loop module is a well known methodology in the literature (such as (Chen 2003), (Bouten 2015)).

While building the networks of loops, two alternative methods of connections can be considered. The first method is connecting adjacent loops with common links and joints and the second method is connection with new joints without any common links or joints. In the second method a new loop is obtained in addition to the two original connected loops. In this Chapter, different deployable networks of modified Altmann linkages are derived and analyzed. Some of the obtained linkages are already published in (Atarer, Korkmaz, and Kiper 2017).

In the following section to construct a network at least two modified Altmann linkages have been used and the mobility of the networks is calculated by using the multi-loop mechanism mobility formula of Alizade (2010):

$$M = \sum_{i=1}^{j} f_i - \sum_{k=1}^{L} \lambda_k + q \tag{45}$$

where j represents the number of joints in the mechanism, f_i represents DoF of the i^{th} joint, L represents the number of independent loops, λ_k is the DoF of space in which loop k operates (λ = 2, 3, etc.) and q is the number of excessive elements (links, joints or loops).

3.1. Network of Modified Altmann Linkages with Common Links or Joints

Advantage of having a common link or joint is that this common member can

reduce the total number of joints and links in the network. In order to obtain a single DoF network by combining single DoF loops, each pair of adjacent loops should have two common links. If the common links are directly connected each other, then the connecting joint will be common in both loops as well. In order to generalize the total number of the joints and links in a network which is constructed by this method, the following formulations can be used:

Total number of links in a network of *n* loops:

$$6n - 2(n-1) = 4n + 2 \tag{46}$$

Total number of joints in a network of *n* loops, if there is a common joint:

$$6n - (n-1) = 5n + 1 \tag{47}$$

Total number of joints is simply 6*n* if there are no common joints. In the following subsections, deployable networks obtained by connecting loops with common links are presented.

3.1.1. Common Bar & Hub Case (Arch Version)

Arch version (Atarer, Korkmaz, and Kiper 2017) can be derived with the combination of two modified Altmann loops with a bar and a hub as two common links and a common joint. As illustrated in Figure 3.1, common links are shown with blue and red colors. In order to calculate the total number of links and joints in the shown network, Eqs. (46)-(47) can be used. For a network of 4 modified Altmann loops (Figure 3.2-Figure 3.3), i.e. $n = 4$, total number of links:

$$n = 4 \Rightarrow 4n + 2 = 4 \times 4 + 2 = 16 \tag{48}$$

total number of joints:

$$n = 4 \Rightarrow 5n + 1 = 5x4 + 1 = 21 \tag{49}$$

The DoF of the network can be calculated according to Eq. (45) with $q = 0$ as

$$M = \sum_{i=1}^{j} f_i - \sum_{k=1}^{L} \lambda_k + q = 21 - 5x4 = 1 \tag{50}$$

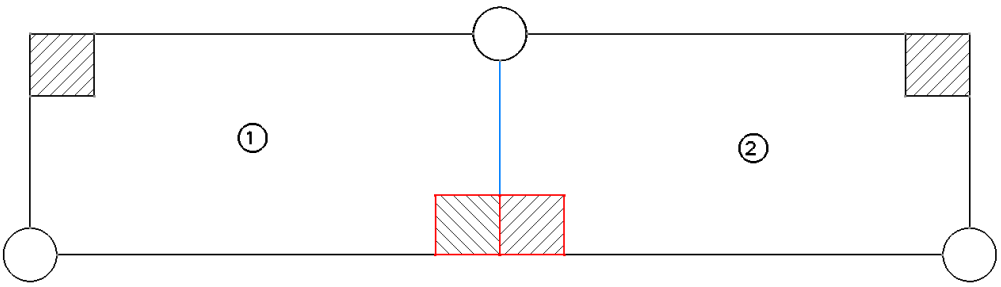

Figure 3.1. Schematic diagram of arch version

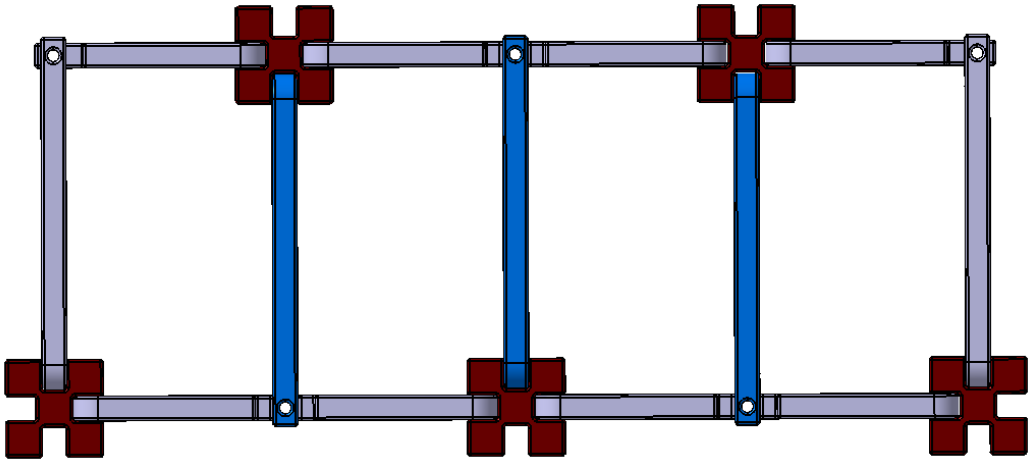

Figure 3.2. Deployed stage of arch version

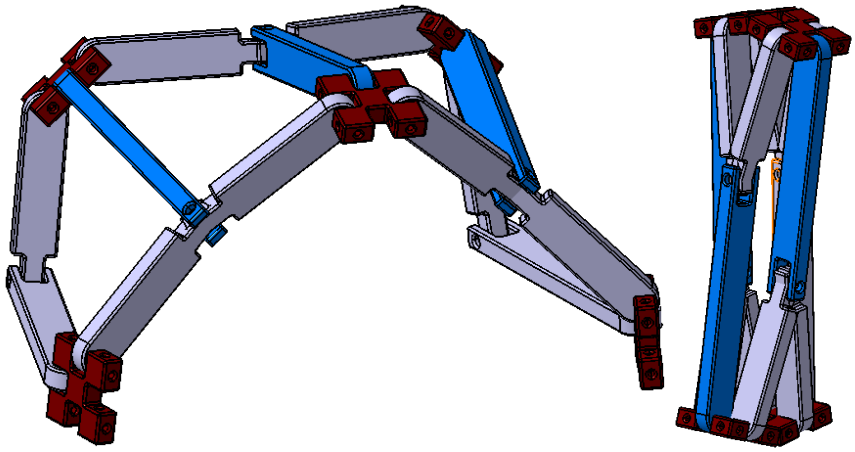

Figure 3.3. Semi-deployed and folded stages of arch version

3.1.2. Common Two Bars Case (Scissor-like Version)

When two bars and a revolute joint is common in adjacent modified Altmann loops, the two bars construct a scissor-like element, hence this network is called as scissor-like version (Atarer, Korkmaz, and Kiper 2017). There are four possible alternatives to construct scissors-like Altmann networks which can be listed as follows:

- Connection of long link to short link
- Connection of short link to short link (or long link to long link)
- Connection of long link to short link with a kink angle
- Connection of short link to short link with a kink angle

The possible networks are is illustrated in Figure 3.4, Figure 3.7, Figure 3.10 and Figure 3.13. In the figures common links are shown with blue and red colors. In order to calculate the total number of links and joints in these networks Eqs. (46)-(47) are used. For a network of 4 modified Altmann loops, i.e. n = 4, total number of links:

$$n = 4 \Rightarrow 4n + 2 = 4 \times 4 + 2 = 18 \tag{51}$$

total number of joints:

$$n = 4 \Rightarrow 5n + 1 = 5x4 + 1 = 21 \tag{52}$$

DoF of these networks does not depend the type of the connection and their mobility can be calculated according to Eq. (45) as

$$M = \sum_{i=1}^{j} f_i - \sum_{k=1}^{L} \lambda_k + q = 21 - 5x4 = 1 \tag{53}$$

The DoF of the network remains 1 with addition of new modules.

3.1.2.1. Connection of Long Link to Short Link

The schematic diagram, deployed, semi-deployed and folded stages of long link

to short link connection type network are respectively illustrated in Figure 3.4-Figure 3.6.

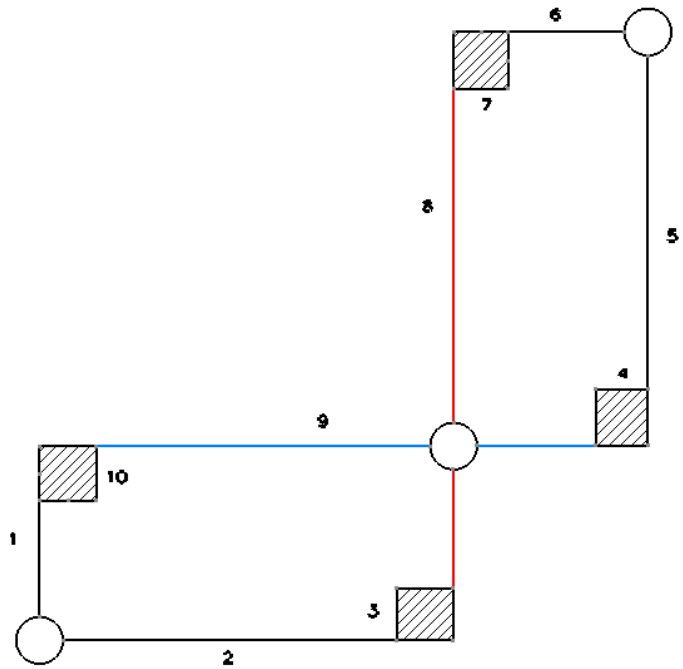

Figure 3.4. Schematic diagram of long link to short link connection

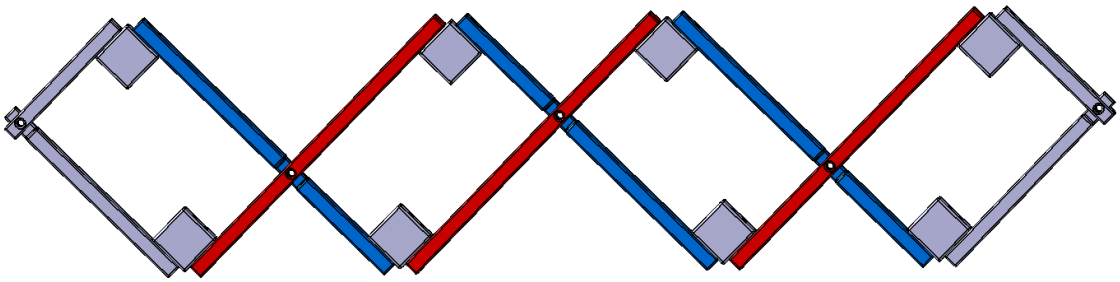

Figure 3.5. Deployed stage of long link to short link connection

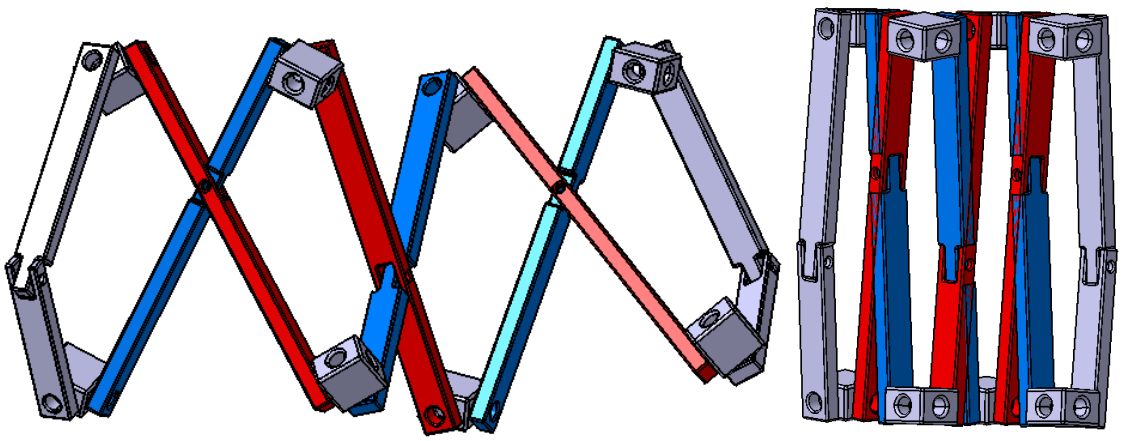

Figure 3.6. Semi-deployed and folded stages of long link to short link connection

3.1.2.2. Connection of Short Link to Short Link (or Long Link to Long Link)

The schematic diagram, deployed, semi-deployed and folded stages of short link to short link connection type network are respectively illustrated in Figure 3.7-Figure 3.9.

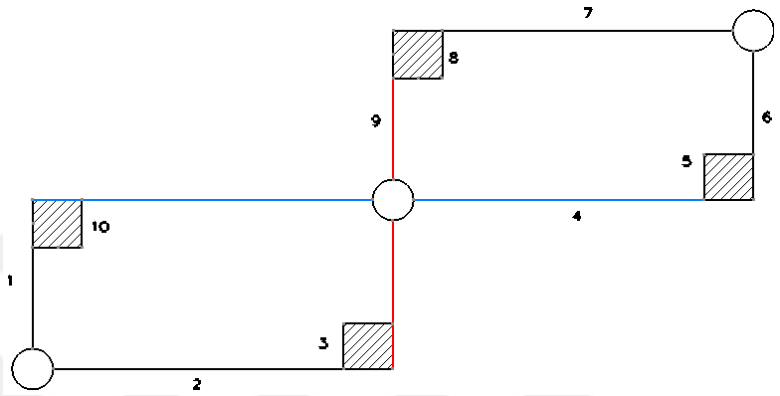

Figure 3.7. Schematic diagram of short link to short link connection

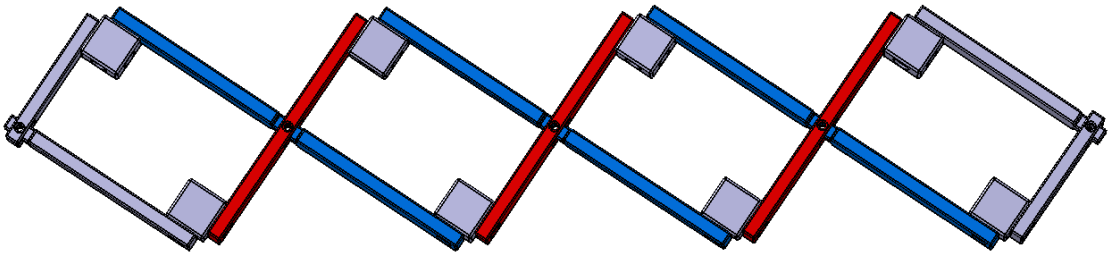

Figure 3.8. Deployed stage of short link to short link connection

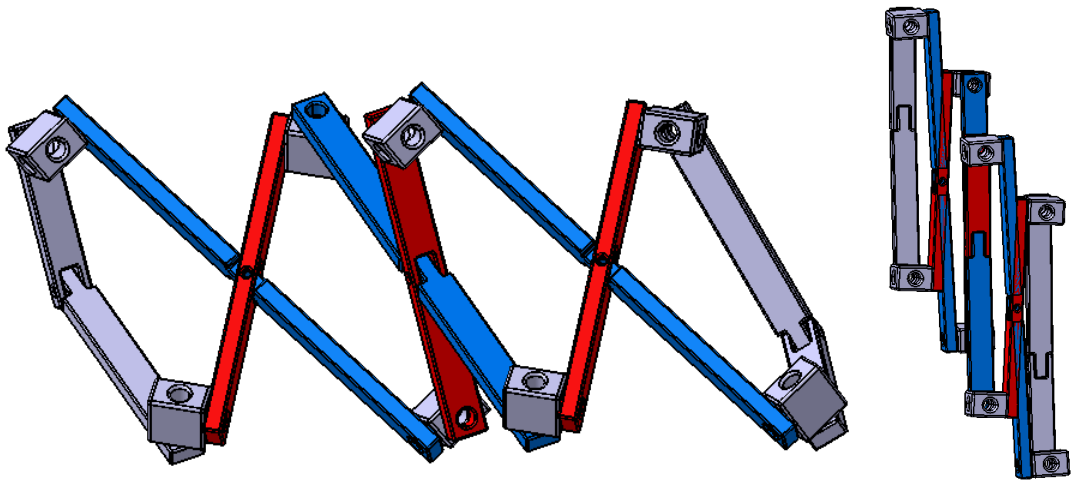

Figure 3.9. Semi-deployed and folded stages of short link to short link connection

3.1.2.3. Connection of Long Link to Short Link with a Kink Angle

The schematic diagram, deployed and semi-deployed stages of long link to short link with a kink angle connection type network are respectively illustrated in Figure 3.10-Figure 3.12.

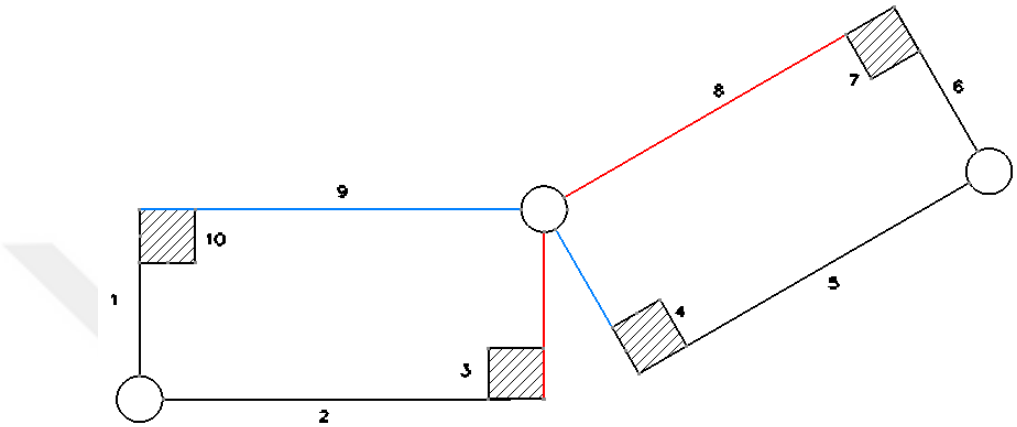

Figure 3.10. Schematic diagram of long link to short link connection with a kink angle

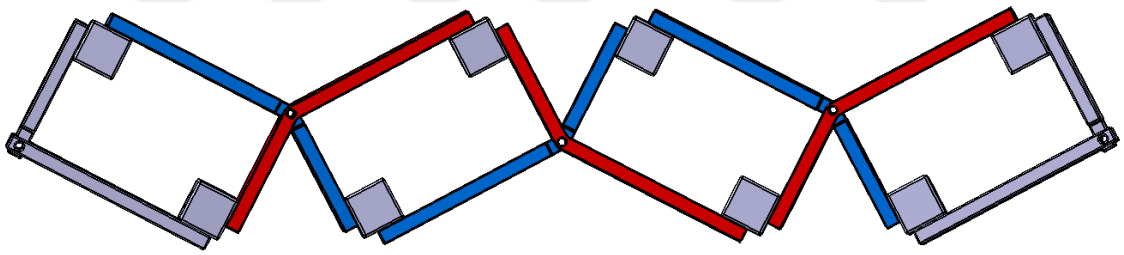

Figure 3.11. Deployed stage of long link to short link connection with a kink angle

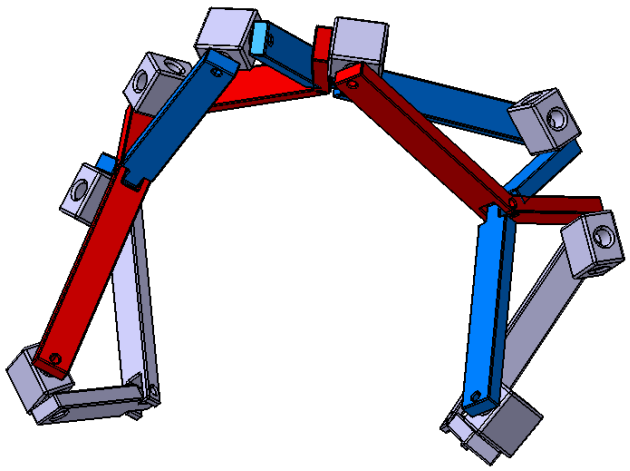

Figure 3.12. Semi-deployed stage of long link to short link connection with a kink angle

3.1.2.4. Connection of Short Link to Short Link (or Long Link to Long Link) with a Kink Angle

The schematic diagram, deployed and semi-deployed stages of short link to short link with a kink angle connection type network are respectively illustrated in Figure 3.13-Figure 3.15. There are two types of networks: 1) with equivalent angulated elements (Figure 3.14), 2) with mirror-image angulated elements in alternating order (Figure 3.15).

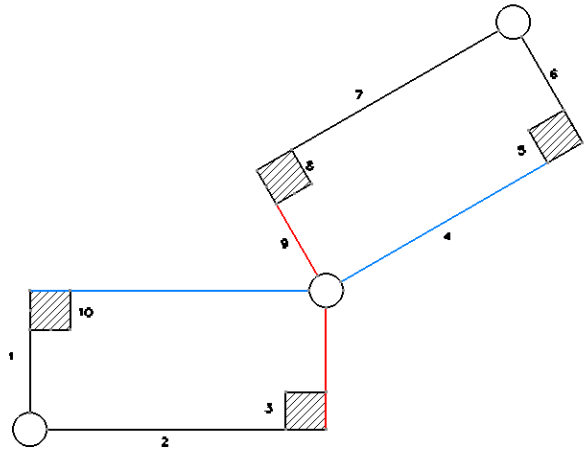

Figure 3.13. Schematic diagram of short link to short link connection with a kink angle

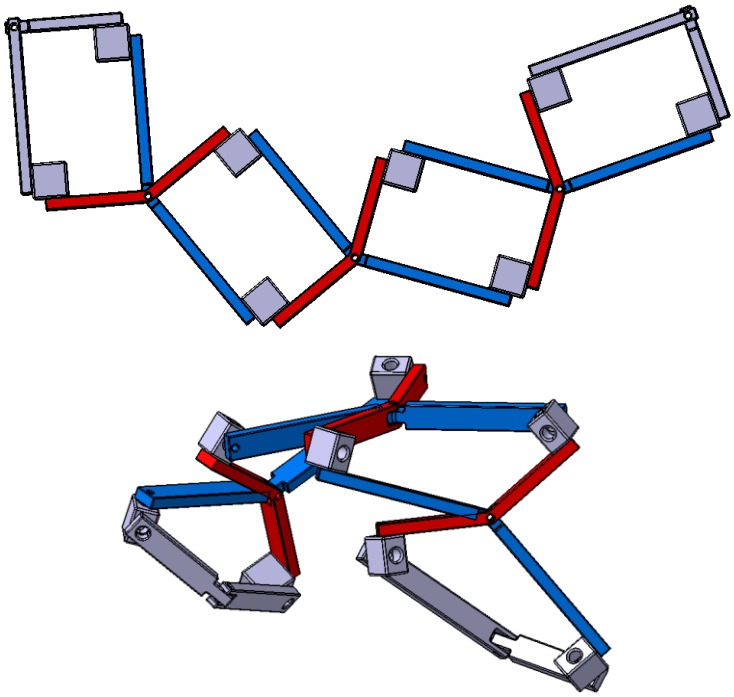

Figure 3.14. Deployed and semi deployed stages of short link to short link connection with a kink angle - with equivalent angulated elements

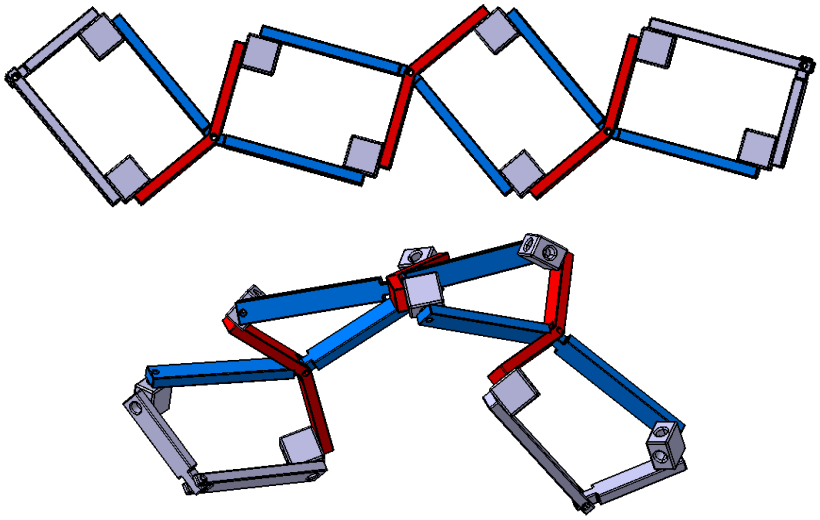

Figure 3.15. Deployed and semi-deployed stages of short link to short link connection with a kink angle - with mirror-image angulated elements

3.1.3. One Common Bar & One Common Hub – New Version

Apart from the arch version, there exists another way to obtain networks with a common bar and a common link. The schematic diagrams of these new networks are illustrated in Figure 3.16 and Figure 3.21. As shown in these figures, common bars are shown with blue color and common hubs are shown in red color. Eqs. (46)-(47) are used to calculate the total number of links and joints in these networks. For a network of 4 modified Altmann loops, i.e. n = 4, total number of links:

$$n = 4 \Rightarrow 4n + 2 = 4 \times 4 + 2 = 18 \tag{54}$$

total number of joints:

$$n = 4 \Rightarrow 5n + 1 = 5x4 + 1 = 21 \tag{55}$$

The DoF of these networks does not depend the type of the connection and their mobility can be calculated according to the Eq. (45) as

$$M = \sum_{i=1}^{j} f_i - \sum_{k=1}^{L} \lambda_k + q = 21 - 5x4 = 1 \tag{56}$$

The DoF of the network remains 1 with addition of new modules.

3.1.3.1. Common Long Link and Hub

The schematic diagram, deployed, semi-deployed and folded stages of common long link and hub connection type network are respectively illustrated in Figure 3.16-Figure 3.20.

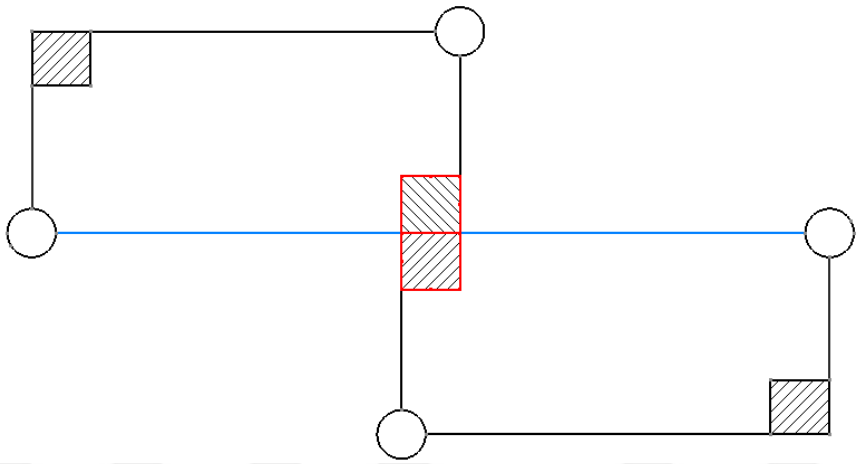

Figure 3.16. Schematic diagram of common long link and hub version

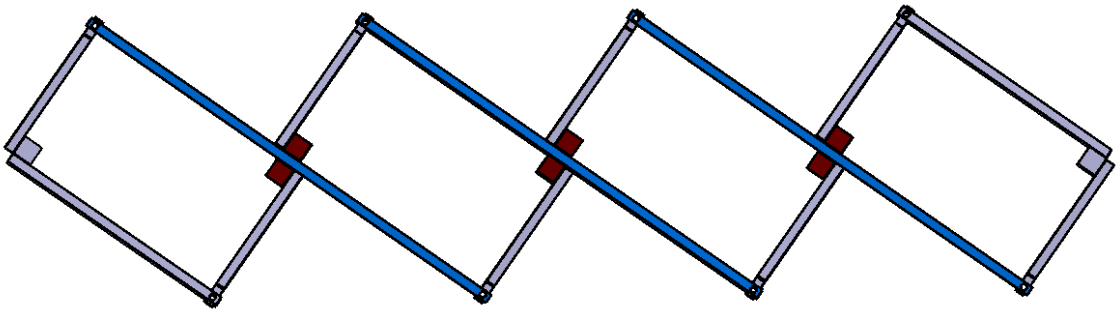

Figure 3.17. Deployed stage of common long link and hub version

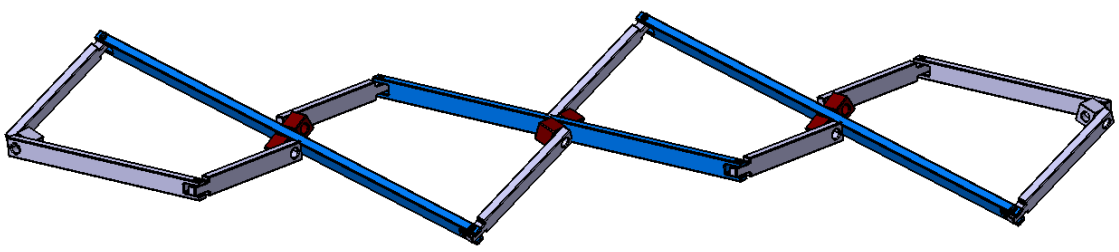

Figure 3.18. Semi-deployed stage of common long link and hub version

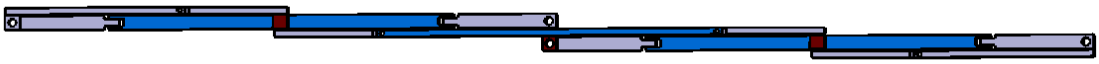

Figure 3.19. Front view of folded stage of common long link and hub version

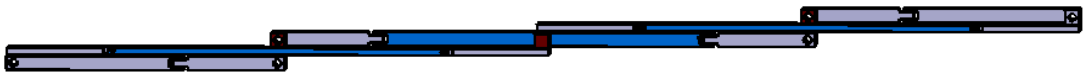

Figure 3.20. Top view of folded stage of common long link and a hub version

3.1.3.2. Common Short Link and Hub

The schematic diagram, deployed, semi-deployed and folded stages of common short link and hub connection type network are respectively illustrated in Figure 3.21-Figure 3.25.

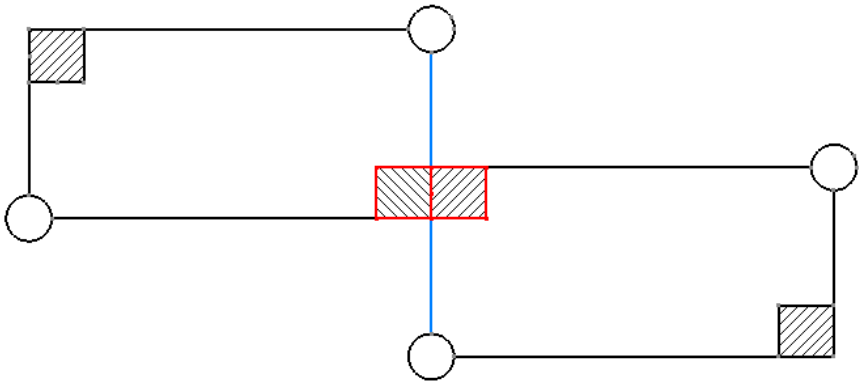

Figure 3.21. Schematic diagram of common short common link and hub version

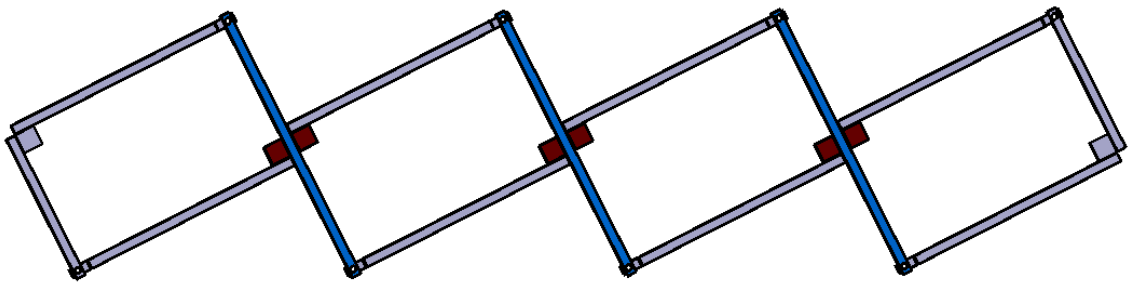

Figure 3.22. Deployed stage of common short common link and hub version

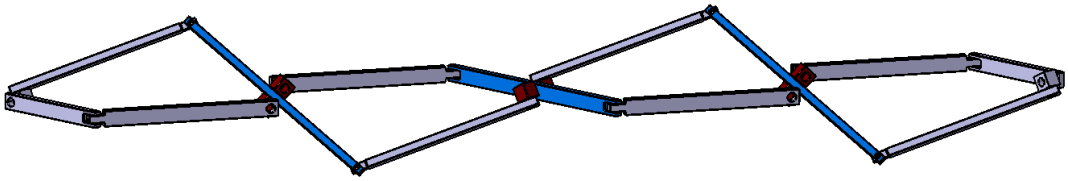

Figure 3.23. Semi-deployed stage of common short common link and hub version

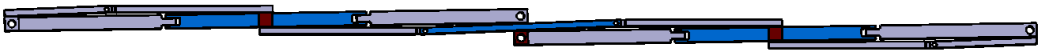

Figure 3.24. Front view of folded stage of common short common link and hub version

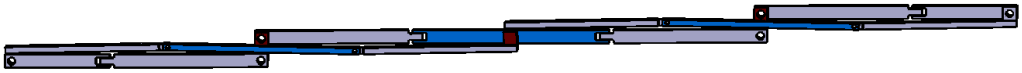

Figure 3.25. Top view of folded stage of common short common link and hub version

3.1.4. Four Loops with a Common Hub (Dome version)

In order to obtain the dome version (Atarer, Korkmaz, and Kiper 2017), four modified Altmann loops should be lapped over by using a common hub, as presented in Figure 3.26. In this case, four loops share a common hub and also adjacent loops share a bar. In this case total number of links and joints differ from the general case, because there is a loop of loops. Total number of links in this network is l = 17 and total number of joints is j = 20. In the previous cases, it was possible to indefinitely add new loops to the network. In this case, only four loops can be connected to each other, so it is a finite network.

While calculating the DoF of this type of network, unlike the previous versions, q is not equal to zero. According to Euler's equation for polyhedra, there are $L = j - l - 1 = 20 - 17 - 1 = 4$ independent loops. According to Eq. (45)

$$M = \sum_{i=1}^{j} f_i - \sum_{k=1}^{L} \lambda_k + q = 20 - 5x4 + 1 = 1 \tag{57}$$

The deployed, semi-deployed and folded stages of the dome version are respectively illustrated in Figure 3.27-Figure 3.28.

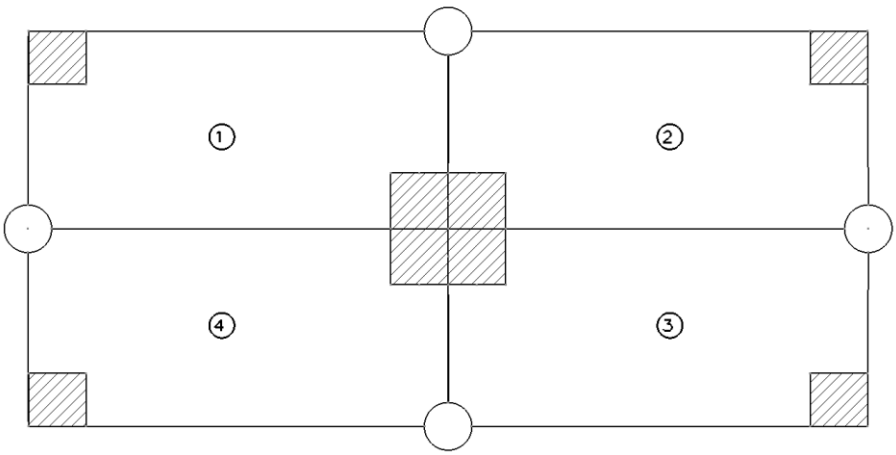

Figure 3.26. Schematic diagram of dome version

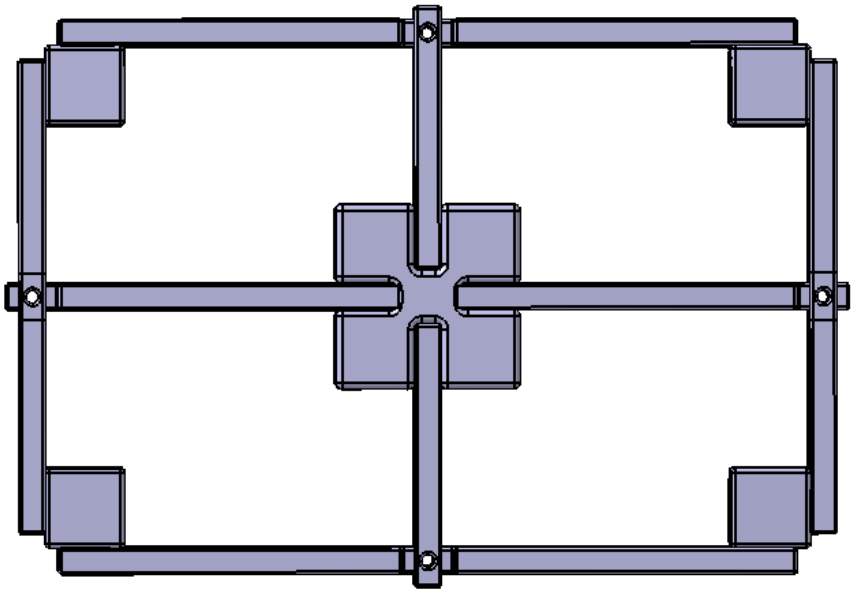

Figure 3.27. Deployed stage of dome version

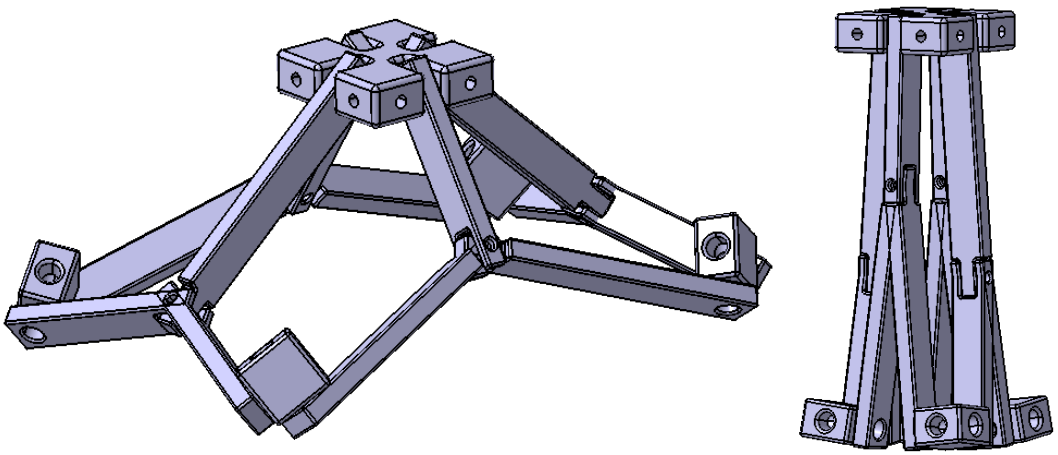

Figure 3.28. Semi-deployed and folded stages of dome version

Kiper (2016) points out that modular deployable structure can be obtained by using dome version and its mirror image, as illustrated in Figure 3.29. The invention can be used to make surfaces composed of planar, spherical, cylindrical or a combination of these geometries, by attaching modules to each other with proper connections. In Figure 3.30, deployed and folded stages of a cylindrical unit is shown.

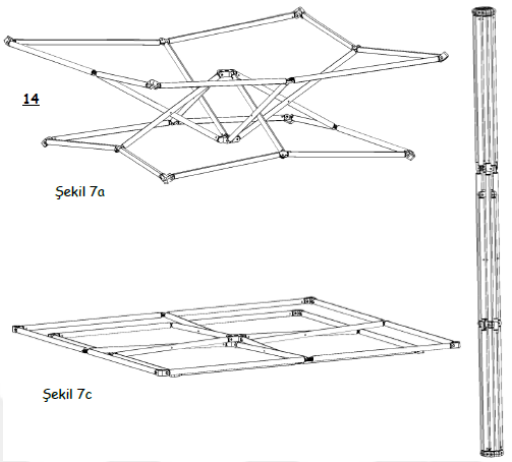

Figure 3.29. Double layer grid unit's deployment stages (Source: Kiper 2016)

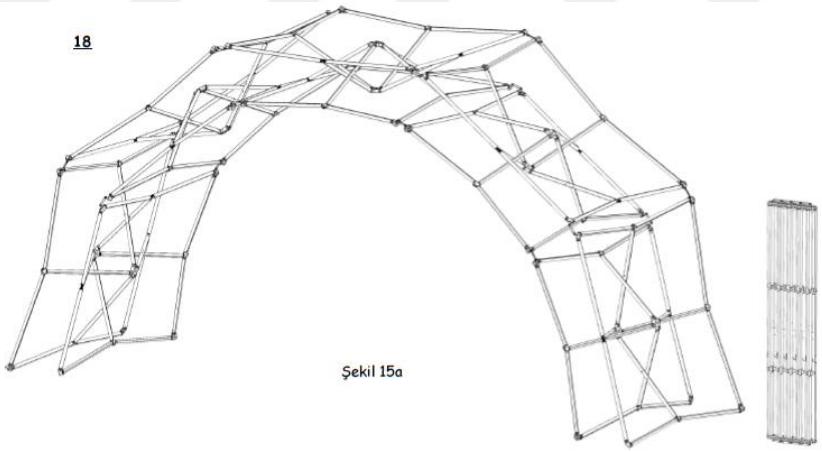

Figure 3.30. Cylindrical unit's deployment stages (Source: Kiper 2016)

3.2. Network of Altmann Linkages with Two New Joints

Three different types of networks are presented in this category. Constructing a new Altmann loop when combining two loops is the first type. Second type is generated by constructing a parallelogram when combining two loops and the third one is combining four loops which constructs two new Altmann and parallelogram loops.

Independent from the network type, while constructing these loops the total number of links in the network of n loops is $6n$. Total number of joints in the first two type of networks can be calculated as

$$6n+2\left(n-1\right)=8n-2 \tag{58}$$

In the case of serial connection of loops total number of independent loops in the network can be found as

$$n+\left(n-1\right)=2n-1 \tag{59}$$

If the loops are connected to construct a loop of loops, the number of independent loops should be obtained using the number of links and joints.

3.2.1. Altmann Loop Version

As illustrated in Figure 3.31-Figure 3.32, when two modified Altmann loops (loops 1 and 3) are connected in the vicinity of U joints with two new revolute joints, a new Altmann loop (loop 2) is generated. For n = 4, total number of links:

$$n=4\Rightarrow 6n=24 \tag{60}$$

total number of joints:

$$n=4\Rightarrow 8n-2=30 \tag{61}$$

Adding a new Altmann linkage adds $q = 2(n - 1)$ excessive elements to the system, and mobility of the network can be calculated according to the Eq. (45) as

$$M=\sum_{i=1}^{j} f_i-\sum_{k=1}^{L}\lambda_k+q=30-5x7+2x(4-1)=1 \tag{62}$$

Networks with new Altmann loops can be generated by connecting a short link to a long link (Figure 3.31) and a long link to a short link (Figure 3.32).

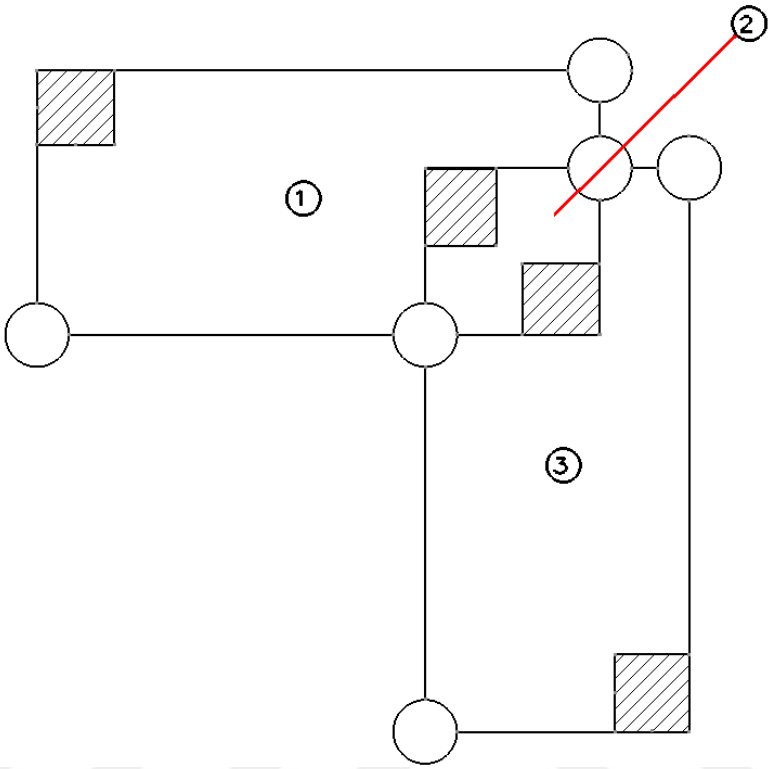

Figure 3.31. Schematic diagram of short link to short link connection

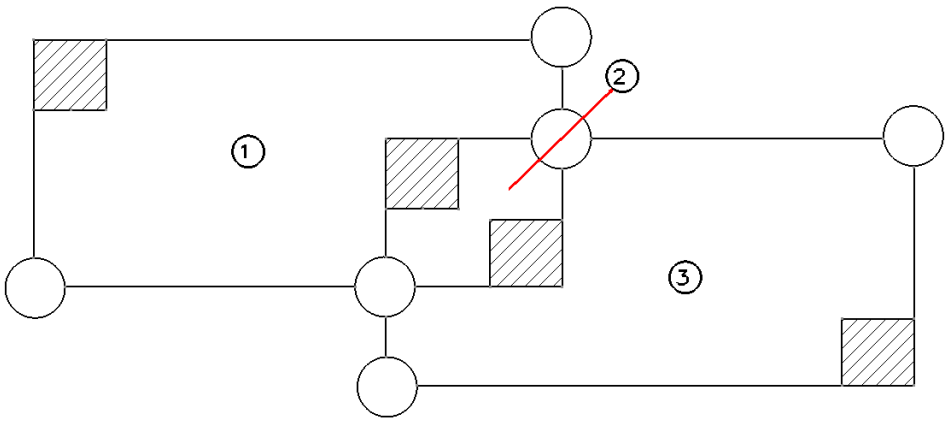

Figure 3.32. Schematic diagram of long link to short link connection

When the dimensions of the links are different ($a \neq b$), the assembly is immobile, because the newly generated Altmann loop cannot be made similar to the original two loops. However, when equilateral Altmann loops ($a = b$) are connected to generate a new equilateral Altmann loop, the network is mobile. This situation is also verified with a CAD model as presented in Figure 3.33-Figure 3.35.

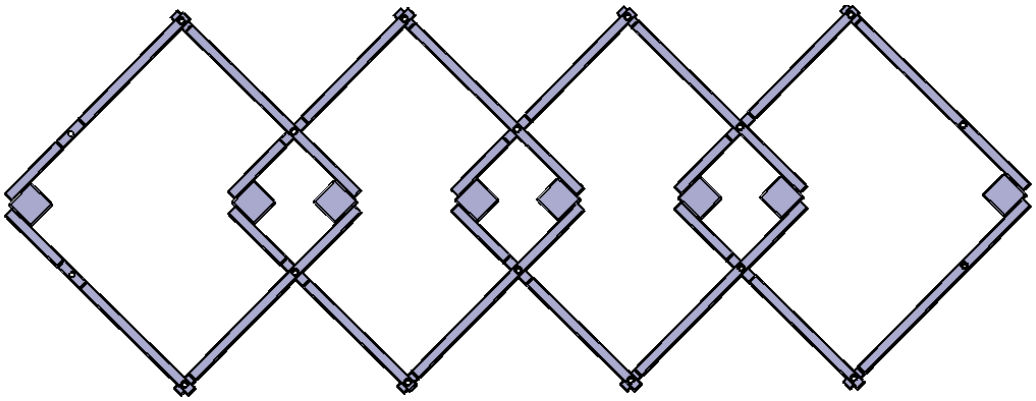

Figure 3.33. Deployed stage of Altmann loop version

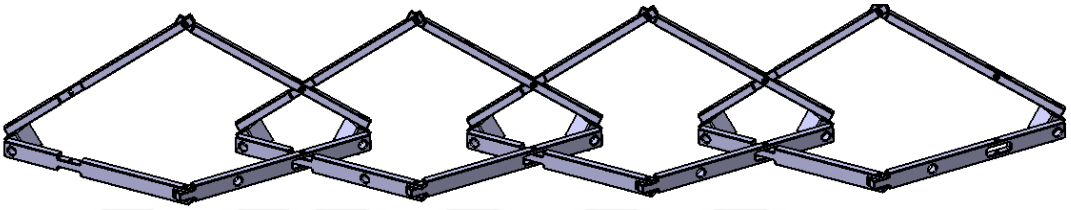

Figure 3.34. Semi-deployed stage of Altmann loop version

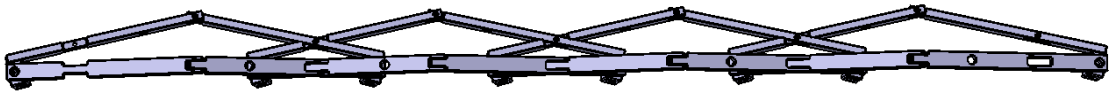

Figure 3.35. Folded stage of Altmann loop version

3.2.2. Parallelogram Loop Version

As presented in Figure 3.36 and Figure 3.39, a parallelogram loop is introduced when two modified Altmann loops are connected to each other in the vicinity of a revolute joint which connects two bars. For n = 4, total number of links:

$$n = 4 \Rightarrow 6n = 24 \tag{63}$$

total number of joints:

$$n = 4 \Rightarrow 8n - 2 = 30 \tag{64}$$

The DoF can be calculated according to Eq. (45):

$$M = \sum_{i=1}^{j} f_i - \sum_{k=1}^{L} \lambda_k + q = 30 - 5x4 - 3x3 = 1 \quad (65)$$

Modified Altmann loops can be connected with new revolute joints connecting a short link of one loop to a long link of the other loop, or with revolute joints connecting short links (or long links) of the two loops. These two cases are examined in the following two sub-sections.

3.2.2.1. Connection of Long Link to Short Link

The schematic diagram, deployed, semi-deployed and folded stages of parallelogram loop version with long link to short link connection type network are respectively illustrated in Figure 3.36-Figure 3.38.

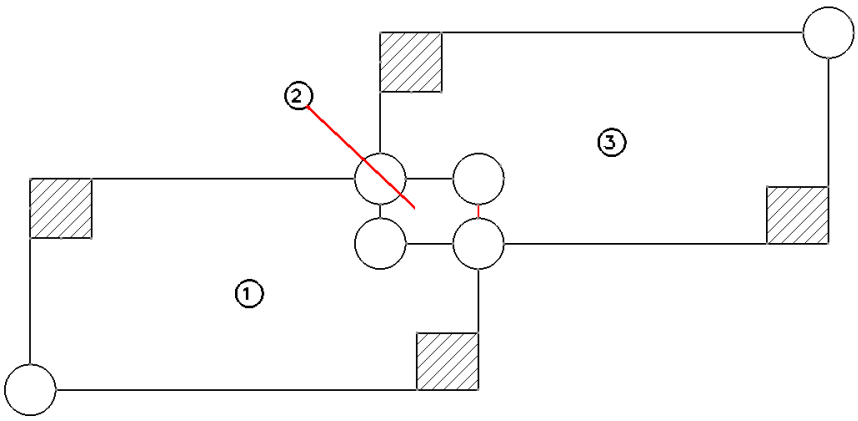

Figure 3.36. Schematic diagram of parallelogram loop version with long link to short link connection

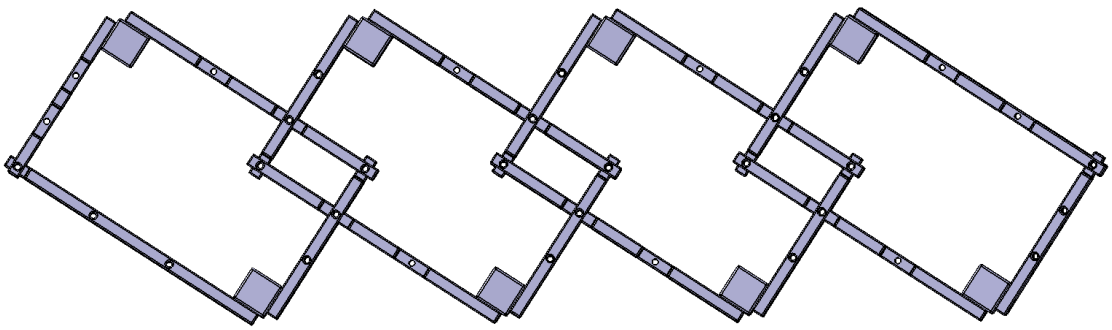

Figure 3.37. Deployed stage of parallelogram loop version with long link to short link connection

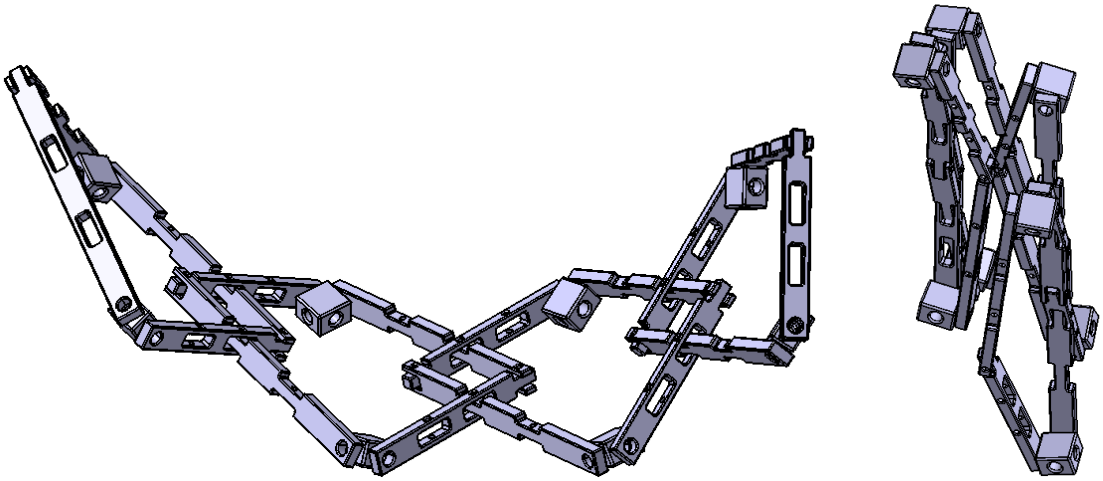

Figure 3.38. Semi-deployed and folded stages of parallelogram loop version with long link to short link connection

3.2.2.2. Connection of Short Link to Short Link

The schematic diagram, deployed, semi-deployed and folded stages of parallelogram loop version with short link to short link connection type network are respectively illustrated in Figure 3.39-Figure 3.41. Figure 3.42-Figure 3.43 illustrates the case with equilateral modified Altmann loops ($a = b$).

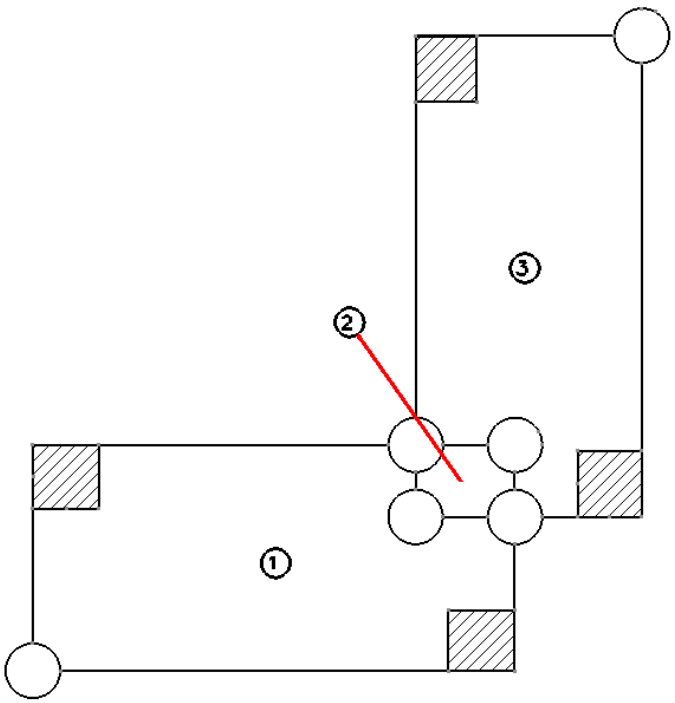

Figure 3.39. Schematic diagram of short link to short link connection

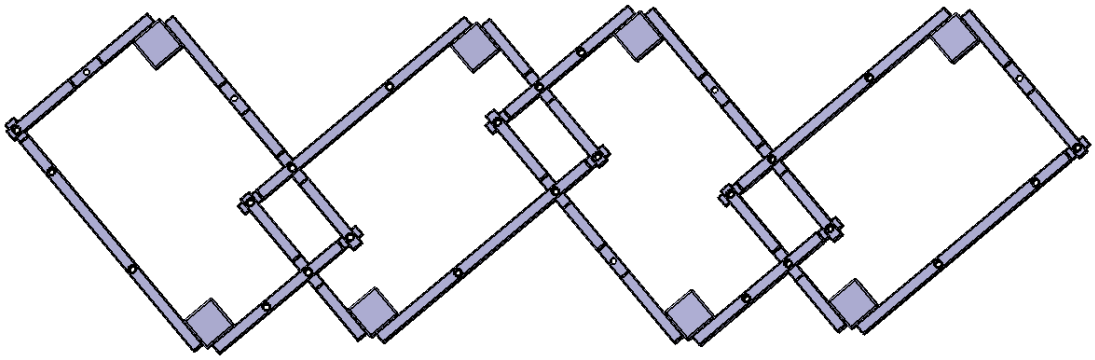

Figure 3.40. Deployed stage of parallelogram loop version with short link to short link connection

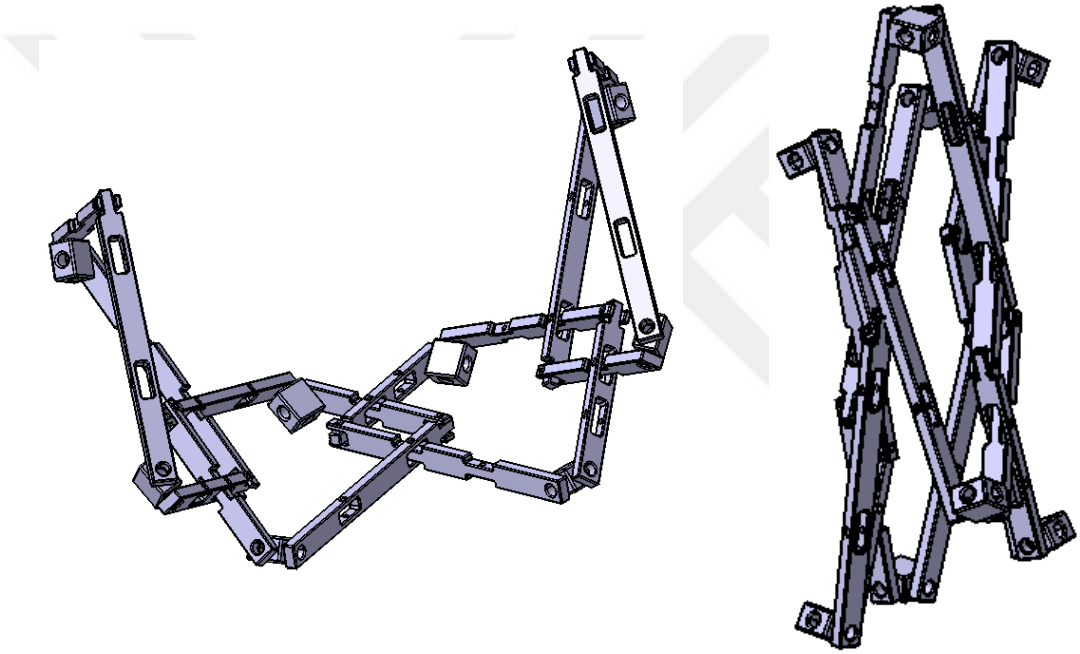

Figure 3.41. Semi-deployed and folded stages of parallelogram loop version with short link to short link connection

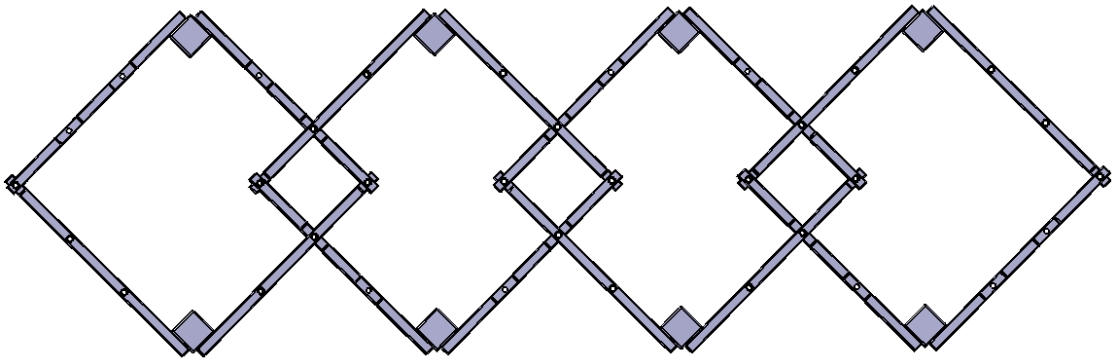

Figure 3.42. Deployed stage of parallelogram loop version when links lengths are equal

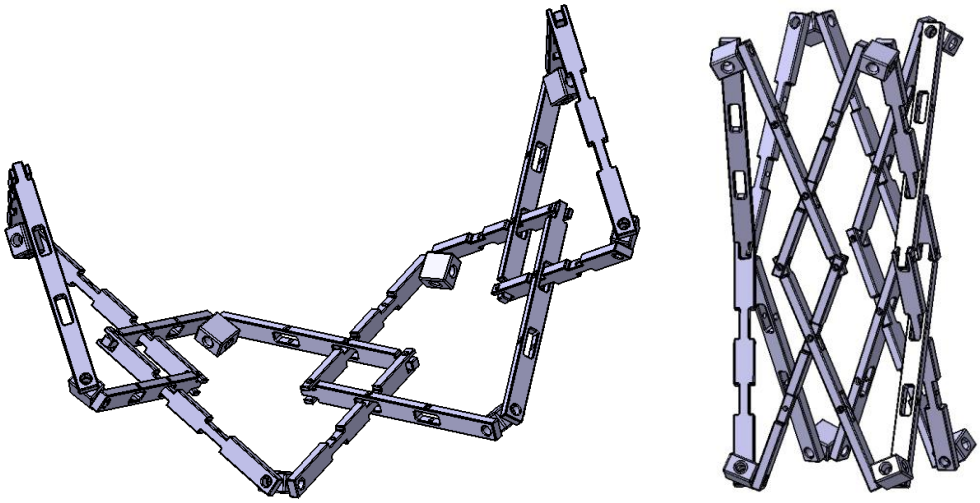

Figure 3.43. Semi-deployed and folded stages of parallelogram loop version when links lengths are equal

3.2.3. 4-Loop Version

In this version four modified Altmann linkages are connected to each other with four pairs of new revolute joints. It is important to notice that if the first connection generates a new Altmann loop, the next loop should be connected to generate a parallelogram loop. Two new Altmann loops and two new parallelogram loops are generated by connecting four modified Altmann loops to obtain a loop of loops (Figure 3.44). This version of network is mobile for equilateral Altmann loops only. For n = 4, total number of links:

$$n = 4 \Rightarrow 6n = 24 \tag{66}$$

Total number of joints in this type of network differs from previous two types. In order to close the loop, 2 extra joints should be added to the network. Therefore, total number of joints in this type of network is

$$n = 4 \Rightarrow 8n - 2 + 2 = 8n = 32 \tag{67}$$

Due to the loop of loops, q = 8 in this case and the DoF can be calculated according to Eq. (45) as

$$M = \sum_{i=1}^{j} f_i - \sum_{k=1}^{L} \lambda_k + q = 32 - 5x6 - 3x3 + 8 = 1 \tag{68}$$

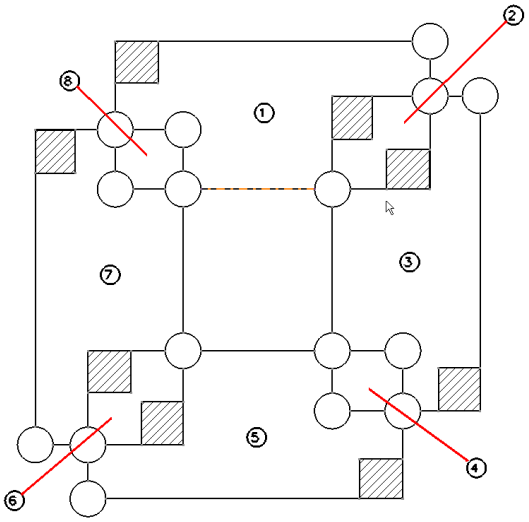

Figure 3.44. Schematic diagram of 4-loop Altmann network

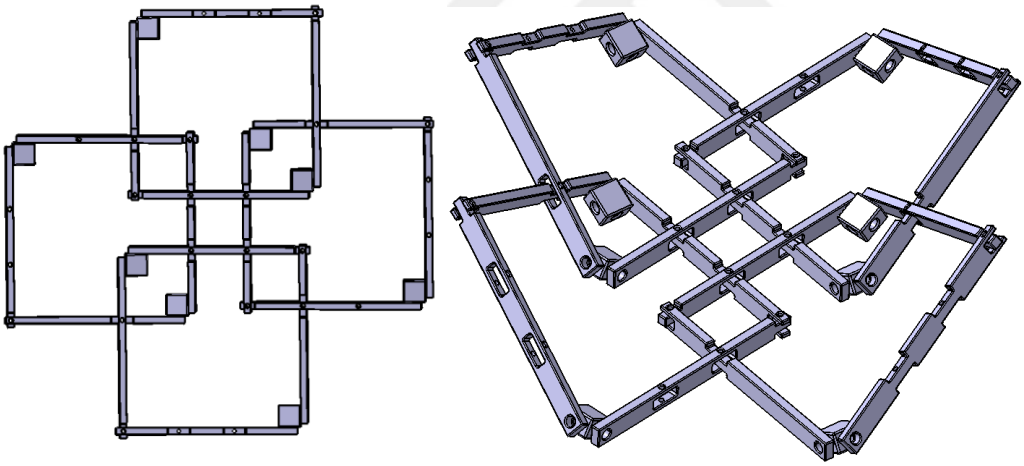

Figure 3.45. Deployed and semi-deployed stages of 4-loop Altmann network

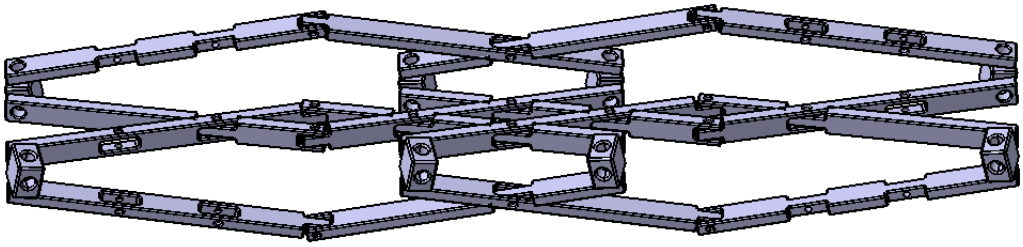

Figure 3.46. Folded stage of 4-loop Altmann network

CHAPTER 4

CONCLUSION

The aim of this thesis study is to perform the kinematic analysis of a modified version of the Altmann linkage and examine possible deployable structures comprising these modified Altmann loops.

The mathematical model of the original Altmann linkage has already been worked out by other researchers. However, the modified version of the Altmann linkage has not been investigated. Within the scope of this thesis, at first the kinematic analysis of modified Altmann linkage is performed to find the relationship between the input and the output parameters of the linkage. Theoretically found results were verified by means of CAD models.

Then, possible alternatives of modified Altmann linkage networks are examined. Some of these networks are already presented in Atarer et al. (2017). In addition to their study, besides equilateral Altmann loops, non-equilateral Altmann loops are also used to construct deployable networks. According to the type of the network, total number of links and joints have been formulated.

When the obtained networks are compared with the networks that have been derived by other researchers, in this thesis, new networks are derived by using different link lengths. These new networks are obtained by combining links that have different/same lengths together and by combining links with kink angles. For the networks that are generated with common links or joints, one new type is obtained, which comprises a common hub and a common bar type of connection.

For the networks that are generated with two new joints, new networks are developed by using different link lengths for the parallelogram loop version. However, Altmann loop version is mobile only for equilateral Altmann loops. Finally, a new type is obtained, which is the 4-loop connection. Whether it is possible to extend this last type of connection to an infinitely large surface is a subject for further studies.

Altmann linkage is a special type of a Bricard general line-symmetric linkage. The modified Altmann linkage issued in this thesis has 4 non-zero joint offsets as opposed to the original Altmann linkage. As further studies, a further modified version with 6 non-

zero joint offsets and link lengths may be investigated. This type of further generalization may lead to easier constructional design for some of the networks presented in this thesis. The networks presented in Chapter 3 may be used to design canopies, tents, roofs, stands, or sunblinds (Atarer et al. 2020). Detailed constructional design, building prototypes and testing the networks obtained in this thesis are further studies that can be conducted.

REFERENCES

Alizade, R. 2010. “Structural synthesis of robot manipulators”. *Proceedings of the International Symposium of Mechanism and Machine Science*.

Altmann, F. G. 1954. “Über raümliche sechsgliedrige Koppelgetriebe,” *Sonderdruck aus der Zeifschrift des Vereines Deutscher Ingenieure* 96(8): 245–249.

Atarer, F. 2019. “Design Alternatives of Network of Altmann Linkages.” Third PhD Thesis Monitoring Report, İzmir Institute of Technology.

Atarer, F., K. Korkmaz, and G. Kiper. 2017. “Design Alternatives of Network of Altmann Linkages.” *International Journal of Computational Methods and Experimental Measurements 5*(4): 495–503.

Atarer, F., Z .T. Kazanasmaz, K. Korkmaz, and G. Kiper. 2020. “The Architectural Application of Altmann Linkage as a Light Shelf.” *Architecture, Technology and Innovation 2020.* İzmir: Yaşar Üniversitesi.

Baker, J. E. 1978. “Overconstrained 5-bars with Parallel Adjacent Joint Axes - II The Linkages.” *Mechanism and Machine Theory* 13(2): 219-233.

Baker, J. E. 1979. “The Bennett, Goldberg and Myard linkages - in Perspective.” *Mechanim and Machine Theory* 14(4): 239–253.

Baker, J. E. 1993. “A Geometrico-Algebraic Exploration of Altmann’s Linkage.” *Mechanism and Machine Theory* 28(2): 249–260.

Baker, J. E., and M. Hu. 1986. “On Spatial Networks of Overconstrained Linkages.” *Mechanism and Machine Theory* 21(5): 427-437.

Beggs, J. S. 1966. *Advanced Mechanism*. New York: Macmillan Company.

Bennett, G. T. 1903. “A New Mechanism.” *Enginnering* 76: 777–778.

Bennett, G. T. 1905. “The Parallel Motion of Sarrus and Some Allied Mechanisms.” *Philosophy Magazine* 54: 803–810.

Bennett, G. T. 1914. “The Skew Isogram Mechanism.” *Proceedings of the London Mathematical Society* 2-13(1): 151–173.

Bouten, S. 2015. “Transformable Structures and their Architectural Application.” MSc Thesis, Universiteit Gent.

Briand, S., and Z. You. 2007. “New Deployable Mechanisms.” Report 2293/07, University of Oxford.

Chen, Y. 2003. “Design of Structural Mechanisms.” PhD Thesis, University of Oxford.

Denavit, J., and R. S. Hartenberg. 1955. “A Kinematic Notation for Lower Pair Mechanisms Based on Matrices.” *ASME Journal of Applied Mechanics* 6: 215-221.

Gogu, G. 2005. “Mobility of Mechanisms: A Critical Review.” *Mechanism and Machine Theory* 40 (9). Elsevier Ltd: 1068–97.

Goldberg, M. 1943. “New Five-Bar and Six-Bar Linkages in Three Dimensions.” *Transactions of ASME* 65: 649–661.

Guo, H., and Z. You. 2012. “Deployable Masts Based on the Bennett Linkage.” *Advances in Reconfigurable Mechanisms and Robots I*, 739–747

Hunt, K. H. 1978. *Kinematic Geometry of Mechanisms*. Oxford: Oxford University Press.

IFToMM Dictionaries Online 2014. http://www.iftomm-terminology.antonkb.nl/, access date: December 14, 2020.

Isaak, R. 2006. “A Study of Overconstrained Linkage Networks.” MSc Thesis, Idaho State University.

Kiper, G. 2016. Katlanabilir Kafes Yapı. Patent No: TR201619595.

Kiper, G. 2018. “ME 573-Deployable Structures.” Lecture note, İzmir Institute of Technology, Izmir, Turkey.

Kiper, G., and E. Söylemez. 2009. “Regular Polygonal and Regular Spherical Polyhedral Linkages Comprising Bennett Loops.” *Proceedings of the 5th International Workshop on Computational Kinematics*, 249–256

Kiper, G., and E. Söylemez. 2010. “Obtaining New Linkages From Jitterbug-Like Polyhedral Linkages.” *AzCIFToMM 2010 - International Symposium of Mechanism and Machine Science*, 137-143.

Liu, S. Y., and Y. Chen. 2009. “Myard Linkage and İts Mobile Assemblies.” *Mechanism*

and Machine Theory 44(10): 1950-1963.

Myard, F. E. 1931. “Contribution à La Géométrie Des Systèmes Articulés.” *Bulletin de La Société Mathématique de France* 59: 183–210.

Phillips, J. 1984. *Freedom in Machinery* (Volume I). Cambridge: Cambridge University Press.

Phillips, J. 1990. *Freedom in Machinery* (Volume II). Cambridge: Cambridge University Press.

Qi, X. Z., Z. Q. Deng, B. Y. Ma, B. Li, and R. Q. Liu. 2011. “Design of Large Deployable Networks Constructed by Myard Linkages.” *Key Engineering Materials* 486: 291-296.

Sarrus, P. T. 1853. “Note Sur La Transformation Des Mouvements Rectilignes Alternatifs, En Mouvements Circulaires, et Reciproquement.” *Comptes Rendus des Séances de l'Académie des Sciences de Paris* 36: 1036.

Song, X., H. Guo, B. Li, R. Liu, and Z. Deng. 2016. “Large Deployable Network Constructed by Altmann Linkages.” *Proceedings of the Institution of Mechanical Engineers, Part C: Journal of Mechanical Engineering Science* 231(2): 341–355.

Söylemez, E. 2011. *Mechanisms*. 4th ed. Middle East Technical University.

Tian, P., and Y. Chen. 2010. “Design of a Foldable Shelter.” In: *Proc. AzCIFToMM 2010 International Symposium of Mechanism and Machine Science*, İzmir, Turkey: 102-106.

Yang, F., J. Li, Y. Chen and Z. You. 2015. “A Deployable Bennett Network in Saddle Surface.” *2015 IFToMM World Congress Proceedings, IFToMM 2015*